Monte Carlo simulation of O(2) ϕ^4 field theory in three dimensions

Peter Arnold

Department of Physics, University of Virginia, P.O. Box 400714, Charlottesville, Virginia 22904-4714

Guy D. Moore

Department of Physics, University of Washington, Seattle, Washington 98195-1560

Using standard numerical Monte Carlo lattice methods, we study non-universal properties of the phase transition of three-dimensional ϕ^4 theory of a two-component real field $\phi = (\phi_1, \phi_2)$ with O(2) symmetry. Specifically, we extract the renormalized values of $\langle \phi^2 \rangle / u$ and r/u^2 at the phase transition, where the continuum action of the theory is $\int d^3x [\frac{1}{2}|\nabla \phi|^2 + \frac{1}{2}r\phi^2 + (u/4!)\phi^4]$. These values have applications to calculating the phase-transition temperature of dilute or weakly interacting Bose gases (both relativistic and nonrelativistic). In passing, we also provide perturbative calculations of various $O(a)$ lattice-spacing errors in three-dimensional O(N) scalar field theory, where a is the lattice spacing.

I. INTRODUCTION

A long-standing problem is how to compute the first correction ΔT_c, due to interactions, to the critical temperature T_c for Bose-Einstein condensation of a very dilute nonrelativistic homogeneous Bose gas in three dimensions. In Ref. [1], we review how this problem is related to three-dimensional O(2) ϕ^4 field theory [2], present the results of lattice simulations of that theory, and so determine ΔT_c. The purpose of the present paper is to provide details of those simulations. The lattice results presented here may also be applied to relativistic Bose gases [3,4] and to nonrelativistic gases in a trapping potential [5].

Three-dimensional O(2) ϕ^4 theory has the continuum action

$$S = \int d^3x \left[\frac{1}{2}|\nabla \phi|^2 + \frac{1}{2}r\phi^2 + \frac{u}{4!}(\phi^2)^2 \right], \qquad (1.1)$$

where $\phi = (\phi_1, \phi_2)$ is a two-component real field and $\phi^2 \equiv \phi_1^2 + \phi_2^2$. For fixed u, we will vary r to reach the second-order critical point $r_c(u)$ of this model. The shift in the critical temperature of a nonrelativistic homogeneous single-species Bose gas is given in terms of this theory by [2]

$$\frac{\Delta T_c}{T_0} = -\frac{2mk_B T_0}{3\hbar^2 n} \Delta \langle \phi^2 \rangle_c, \qquad (1.2)$$

where m is the boson mass, n is the number density, and

$$\Delta \langle \phi^2 \rangle_c \equiv [\langle \phi^2 \rangle_c]_u - [\langle \phi^2 \rangle_c]_0 \qquad (1.3)$$

represents the difference between the critical-point value of $\langle \phi^2 \rangle$ for the cases of (i) u non-zero and (ii) the ideal gas $u = 0$ (with $r \to 0$ from above). The result for $\Delta \langle \phi^2 \rangle_c$ in the O(2) theory (1.1) can only depend on u and so, by dimensional analysis, it must be proportional to u. A primary goal will be to discuss in detail the measurement of the numerical constant $\Delta \langle \phi^2 \rangle_c / u$ from lattice Monte Carlo simulations of the theory. As reported in Ref. [1], our result is

$$\frac{\Delta \langle \phi^2 \rangle_c}{u} = -0.001\,198 \pm 0.000\,017. \qquad (1.4)$$

The critical value r_c of r is also useful for various theoretical applications, such as determining corrections to the value of the chemical potential at the transition [5], or to the critical temperature of a trapped gas [5], or to the critical temperature of ultrarelativistic ϕ^4 theory at zero chemical potential [4]. The ϕ^2 interaction is associated with an ultraviolet (UV) divergence of the three-dimensional theory and so must be renormalized. If one chooses the renormalization scale $\bar{\mu}$ to be of order u then, by dimensional analysis, the renormalized value of $r_c(\bar{\mu})$ must be proportional to u^2. The precise scheme used to renormalize r, and the precise choice of $\bar{\mu}$, is a matter of convention. In this paper, we will report a measurement of the numerical constant r_c/u^2 for r defined by dimensional regularization and modified minimal subtraction ($\overline{\text{MS}}$) at a renormalization scale of $\bar{\mu} = u/3$. Our result is

$$\frac{r_c^{\overline{\text{MS}}}(u/3)}{u^2} = 0.001\,920\,1 \pm 0.000\,002\,1. \qquad (1.5)$$

One may convert to other choices of $\bar{\mu}$ by the (exact) identity

$$\frac{r^{\overline{\text{MS}}}(\bar{\mu}_1)}{u^2} = \frac{r^{\overline{\text{MS}}}(\bar{\mu}_2)}{u^2} + \frac{2}{9(4\pi)^2} \ln \frac{\bar{\mu}_1}{\bar{\mu}_2}. \qquad (1.6)$$

In Sec. II, we discuss the lattice action we use, its relationship to continuum fields and parameters, how we correct for $O(a)$ lattice spacing errors, and the algorithms we use for simulation. Section III details our procedure for finding the transition, based on the method of Binder cumulants. In Sec. IV, we present our initial data, show that we have simulated moderately large volumes, and then discuss how to analyze the remaining finite-volume corrections by making use of the known critical exponents associated with this universality class. The corresponding numerical extrapolations of the finite-volume corrections are given in Sec. V. Numerical ex-

trapolation of the continuum limit is presented in Sec. VI. A table of all our raw data for various size lattices and values of coupling may be found in Appendix A. The derivations of the $O(a)$ lattice-spacing corrections used in this paper are given in Appendix B. The remaining appendices include various discussions of scaling laws used in the text, an analytic calculation of results for small lattice volumes, and a critical discussion of one of the early simulations, in the literature, of the Bose-Einstein condensation temperature of dilute nonrelativistic gases.

II. LATTICE ACTION, MEASUREMENT, AND ALGORITHM

The bare lattice Lagrangian has the form

$$\mathcal{L} = a^3 \sum_{\mathbf{x}} \left[\frac{1}{2} (-\Phi_1 \boldsymbol{\nabla}_{\text{lat}}^2 \Phi_1 - \Phi_2 \boldsymbol{\nabla}_{\text{lat}}^2 \Phi_2) + \frac{r_0}{2} (\Phi_1^2 + \Phi_2^2) \right.$$
$$\left. + \frac{u_0}{4!} (\Phi_1^2 + \Phi_2^2)^2 \right], \qquad (2.1)$$

where a is the lattice spacing. In an actual simulation, one invariably chooses lattice units where $a=1$, or equivalently works with rescaled fields and parameters $\Phi^{\text{L}} = a^{1/2}\Phi$, $r_0^{\text{L}} = a^2 r_0$, and $u_0^{\text{L}} = a u_0$. For the sake of presentation, however, we will generally avoid specializing to lattice units.

We work on a simple cubic lattice, and will work in cubic volumes $L \times L \times L$ with periodic boundary conditions, corresponding to $(L/a)^3$ sites. The simplest possible implementation of the lattice Laplacian, which we call the "unimproved" choice ∇_{U}^2, would be

$$\nabla_{\text{U}}^2 \Phi(\mathbf{x}) = a^{-2} \sum_{\mathbf{i}} [\Phi(\mathbf{x}+a\mathbf{i}) - 2\Phi(\mathbf{x}) + \Phi(\mathbf{x}-a\mathbf{i})],$$
$$(2.2)$$

where the sum is over unit vectors in the three lattice directions: (1,0,0), (0,1,0), and (0,0,1). We use instead a standard improvement, which approaches the continuum Laplacian faster for smooth fields

$$\nabla_{\text{I}}^2 \Phi(\mathbf{x}) = a^{-2} \sum_{\mathbf{i}} \left[-\tfrac{1}{12}\Phi(\mathbf{x}+2a\mathbf{i}) + \tfrac{4}{3}\Phi(\mathbf{x}+a\mathbf{i}) - \tfrac{5}{2}\Phi(\mathbf{x}) \right.$$
$$\left. + \tfrac{4}{3}\Phi(\mathbf{x}-a\mathbf{i}) - \tfrac{1}{12}\Phi(\mathbf{x}-2a\mathbf{i}) \right]. \qquad (2.3)$$

The difference can be seen from the Fourier transforms of the operators ∇_{U}^2 and ∇_{I}^2, which are

$$\widetilde{k}_{\text{U}}^2 \equiv a^{-2} \sum_{i} [2 - 2\cos(ak_i)], \qquad (2.4)$$

$$\widetilde{k}_{\text{I}}^2 \equiv a^{-2} \sum_{i} \left(\frac{5}{2} - \frac{8}{3}\cos(ak_i) + \frac{1}{6}\cos(2ak_i) \right), \quad (2.5)$$

and have small k limits

$$\widetilde{k}_{\text{U}}^2 = k^2 + O(a^2 k^4), \qquad (2.6)$$

$$\widetilde{k}_{\text{I}}^2 = k^2 + O(a^4 k^6). \qquad (2.7)$$

The unimproved Laplacian has $O(a^2)$ error, while the improved Laplacian has only $O(a^4)$ errors.

A. An unimproved calculation of $\Delta \langle \phi \rangle^2$

One of our tasks is to calculate the continuum ratio $\Delta \langle \phi^2 \rangle / u$. In the lattice theory (2.1), the free field ($u_0 = 0$) result for $\langle \Phi^2 \rangle$ is

$$\langle \Phi^2 \rangle_{u_0=0} = \langle \Phi_1^2 + \Phi_2^2 \rangle_{u_0=0} = 2 \int_{\mathbf{k} \in \text{BZ}} \frac{1}{\widetilde{k}^2}, \qquad (2.8)$$

where the integral is over the Brillouin zone $|k_i| \leq \pi/a$. Scaling out the dependence on a, we define

$$\frac{\Sigma}{4\pi a} \equiv \int_{\mathbf{k} \in \text{BZ}} \frac{1}{\widetilde{k}^2}. \qquad (2.9)$$

For the improved Laplacian, we obtain the value of the constant Σ by numerical integration

$$\Sigma \simeq 2.752\,383\,911\,207\,52. \qquad (2.10)$$

On the lattice, the most straightforward implementation of the ratio $\Delta \langle \phi^2 \rangle / u$ is then

$$\frac{\Delta_0 \langle \Phi^2 \rangle}{u_0} \equiv \frac{1}{u_0} \left[\langle \Phi^2 \rangle - \frac{2\Sigma}{4\pi a} \right]. \qquad (2.11)$$

This will approach the desired continuum value as $ua \to 0$, but the lattice spacing errors at small ua will be $O(ua)$.

B. Relationship between lattice and continuum fields and parameters

One of our goals will be to reduce finite lattice-spacing errors, so that we may obtain better estimates of the continuum limit with a given coarseness of lattice. To eliminate errors at a given order in a, one must not only improve the form of the Laplacian but must also perform an appropriate calculation of the relationship between lattice and continuum parameters. To this end, we will rewrite our bare lattice action in terms of continuum fields ϕ and parameters (r,u) as

$$\mathcal{L} = a^3 \sum_{\mathbf{x}} \left[\frac{Z_\phi}{2} (-\phi_1 \boldsymbol{\nabla}_{\text{lat}}^2 \phi_1 - \phi_2 \boldsymbol{\nabla}_{\text{lat}}^2 \phi_2) \right.$$
$$\left. + \frac{Z_r(r+\delta r)}{2} (\phi_1^2 + \phi_2^2) + \frac{u+\delta u}{4!} (\phi_1^2 + \phi_2^2)^2 \right], \qquad (2.12)$$

where the renormalizations Z_ϕ, Z_r, δr, and δu will only depend on ua at the order of interest. We explain their derivation in Appendix B. For continuum r defined by $\overline{\text{MS}}$ renormalization at a scale $\bar{\mu}$, we find

$$Z_\phi = 1 + \frac{2C_2}{9} \frac{(ua)^2}{(4\pi)^2} + O((ua)^3), \qquad (2.13a)$$

$$Z_r = 1 + \frac{2\xi}{3} \frac{ua}{(4\pi)} + \left(\frac{4\xi^2}{9} - \frac{2C_1}{3}\right)\frac{(ua)^2}{(4\pi)^2} + O((ua)^3),$$

$$(2.13b)$$

$$\delta r = a^{-2}\left[-\frac{2\Sigma}{3}\frac{(ua)}{(4\pi)} + \frac{2}{9}\left(\ln\frac{6}{\bar{\mu}a} + C_3 - 3\Sigma\xi\right)\frac{(ua)^2}{(4\pi)^2}\right.$$

$$\left. + O((ua)^3)\right],$$

$$(2.13c)$$

$$\delta u = a^{-1}\left[\frac{5\xi}{3}\frac{(ua)^2}{(4\pi)} + \left(-\frac{32C_1}{9} + \xi^2\right)\frac{(ua)^3}{(4\pi)^2} + O((ua)^4)\right],$$

$$(2.13d)$$

where we have introduced several more numerical constants, given by various integrals in lattice perturbation theory, whose values (for the action with the improved Laplacian) are approximately

$$\xi \simeq -0.083\,647\,053\,040\,968, \qquad (2.14a)$$

$$C_1 \simeq 0.055\,061\,2, \qquad (2.14b)$$

$$C_2 \simeq 0.033\,416, \qquad (2.14c)$$

$$C_3 \simeq -0.861\,479\,16. \qquad (2.14d)$$

One needs to similarly match the operator ϕ^2 whose expectation is taken in determining $\Delta\langle\phi^2\rangle$. In Appendix B, we discuss the relationship between the continuum and lattice operators and show that the continuum result for $\Delta\langle\phi^2\rangle$ is

$$\Delta\langle\phi^2\rangle = Z_r\langle\phi^2\rangle_{\text{lat}} - \delta\phi^2 + O(a^2), \qquad (2.15)$$

where the constant $\delta\phi^2$ is

$$\delta\phi^2 = a^{-1}\left\{\frac{2\Sigma}{4\pi} + \frac{4\xi\Sigma}{3}\frac{ua}{(4\pi)^2} + \frac{4}{9}[C_4 - 3\Sigma C_1 - \Sigma C_2\right.$$

$$\left. + 2\xi^2\Sigma + \xi\ln(\bar{\mu}a)]\frac{(ua)^2}{(4\pi)^3} - \xi\frac{ra^2}{4\pi}\right\}. \qquad (2.16)$$

The additional numerical constant is

$$C_4 \simeq 0.282. \qquad (2.17)$$

We note in passing that the logarithm in Eq. (2.16) represents the explicit subtraction of an effect analogous to a [quadratic × logarithmic] correction to the critical temperature for Bose condensation of dilute nonrelativistic gases, discussed in Ref. [7]. In this analogy, the lattice spacing a in our simulation plays a role similar to the thermal wavelength in the Bose condensation problem, and u and $\bar{\mu}$ (which is chosen of order u) are proportional to the scattering length.

In this paper, whenever we quote simulation results for a given value of ua and ra^2, we are referring to simulations of the action (2.12) with parameters given by Eqs. (2.13) and (2.15) with $O(\cdots)$ set to zero. When we quote values of $\Delta\langle\phi^2\rangle_c$, we will be quoting continuum values, as given by
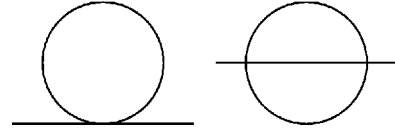

FIG. 1. The two fundamental UV-divergent graphs of continuum ϕ^4 theory.

Eq. (2.15). This will be adequate to reduce the lattice-spacing error to $O(a^2)$ on individual measurements of $\Delta\langle\phi^2\rangle_c/u$ and to $O(a)$ on individual measurements of r_c.

The precise definition of continuum r, and its relationship to bare lattice r_0, are in principle unnecessary if one's interest is only to determine $\Delta\langle\phi^2\rangle_c$—one could simply find the critical value of r_0 at any given lattice spacing and not worry about its relation to continuum definitions. However, as a practical matter, knowing the relationship facilitates using results at one lattice spacing to make a good initial guess of the critical value of r_0 at another lattice spacing. And, as discussed earlier, the continuum critical value of r is of interest in its own right.

Throughout this paper, continuum r should be understood as defined by $\overline{\text{MS}}$ renormalization at a renormalization scale $\bar{\mu}$. That is, the continuum Lagrangian is the $\epsilon \to 0$ limit of the $(3-\epsilon)$-dimensional action

$$S = \int d^{3-\epsilon}x\left[\frac{1}{2}Z_\phi|\nabla\phi|^2 + \frac{1}{2}r_{\text{bare}}\phi^2 + \mu^\epsilon\frac{u_{\text{eff}}}{4!}(\phi^2)^2\right],$$

$$(2.18)$$

with the bare continuum parameter r_{bare} related to the renormalized $r = r_{\overline{\text{MS}}}(\bar{\mu})$ by

$$r_{\text{bare}} = r + \frac{1}{(4\pi)^2\epsilon}\left(\frac{u}{3}\right)^2, \qquad (2.19)$$

and with

$$\mu \equiv \frac{e^{\gamma_E/2}}{\sqrt{4\pi}}\bar{\mu}. \qquad (2.20)$$

[The factor of $e^{\gamma_E/2}/\sqrt{4\pi}$ in Eq. (2.20) is what distinguishes modified minimal subtraction ($\overline{\text{MS}}$) from unmodified minimal subtraction (MS); the difference between the two schemes amounts to nothing more than a multiplicative redefinition of the renormalization scale. The constant $\gamma_E = 0.5772\ldots$ is Euler's constant.] Three-dimensional ϕ^4 theory is super renormalizable and the only fundamental UV divergences of the continuum theory are those corresponding to the two diagrams of Fig. 1. The first has a linear divergence, which is ignored by dimensional regularization. The second has a logarithmic divergence, which is the origin of the u^2/ϵ counter-term present in Eq. (2.19).

C. Algorithm

We evolve configurations in Monte Carlo time using a combination of site-by-site heatbath and multigrid [8] over-relaxation updates.

In Sec. III, we discuss how we define a nominal value of the location r_c of the transition in finite volume. In order to scan for the transition, we need to be able to smoothly vary r. We use the standard technique of canonical reweighting. Having made a simulation at one value r_{sim} of r, and accumulated a Monte Carlo time series of values of

$$\overline{\phi^2} \equiv \frac{1}{V} \int d^3x \, \phi^2(\mathbf{x}), \qquad (2.21)$$

expectations at nearby values $r = r_{sim} + \delta r$ can be calculated as

$$\langle \mathcal{O} \rangle_r = \frac{\left\langle \exp\left(-\frac{1}{2}V\delta r \overline{\phi^2}\right) \mathcal{O} \right\rangle_{r_{sim}}}{\left\langle \exp\left(-\frac{1}{2}V\delta r \overline{\phi^2}\right) \right\rangle_{r_{sim}}}. \qquad (2.22)$$

We estimate our statistical errors for the estimates of r_c and $\Delta\langle\phi^2\rangle_c$ in a given simulation run using the jackknife method with 20 bins. The size of the bins must be large compared to the decorrelation time, and this is verified in Appendix A, where we quote decorrelation times and sample sizes for each of our simulations.

III. FINDING THE CRITICAL POINT

Systems only have sharply defined phase transitions in infinite volume, but we use the method of Binder cumulants [9] to obtain a good estimate, in finite-volume simulations, of the critical value r_c of r. Specifically, we measure the cumulant

$$C = \frac{\langle \overline{\phi}^4 \rangle}{\langle \overline{\phi}^2 \rangle^2} \qquad (3.1)$$

as a function of r, where the two-component vector $\overline{\phi}$ is the volume average of ϕ

$$\overline{\phi} \equiv \frac{1}{V} \int d^3x \, \phi(\mathbf{x}). \qquad (3.2)$$

In infinite volume, the cumulant C is one in the ordered phase and two in the disordered phase. In large volume, there is a smooth transition between these two values, and the width of the transition region shrinks as the volume is increased. Specifically, for an $L \times L \times L$ volume, the width in r of the transition region scales as L^{-y_t} in the $L \to \infty$ limit, where $y_t = 1/\nu$ and ν is the correlation-length critical exponent. The value of the exponent is

$$y_t \equiv 1/\nu \simeq 1.49 \qquad (3.3)$$

for the universality class of the O(2) model.[1]

One method of estimating the location of the transition in finite volume is to simply choose a fixed value C_* of C between one and two and then define the nominal r_c in finite volume as the r for which $C(r) = C_*$. This leads to errors in r_c (contributing to errors in other quantities measured at the transition) that would scale away as L^{-y_t} in the large L limit. This L^{-y_t} scaling of finite-size errors is typical of many prescriptions for defining r_c in finite volume.

The method of Binder cumulants improves the scaling of the finite-size error in r_c from L^{-y_t} to $L^{-y_t-\omega}$, where ω is the critical exponent associated with corrections to scaling, and

$$\omega \simeq 0.79 \qquad (3.4)$$

for the universality class of the O(2) model.[2] One version of the method is to measure the curves $C(r)$ for two different large system sizes L_1 and L_2, and then estimate r_c as the point $r_\times$ where the curves intersect. Specifically, Binder [9] showed that, in the $L_1, L_2 \to \infty$ limit, the error scales as

$$r_\times(L_1, L_2) - r_c \sim \frac{L_2^{-\omega} - L_1^{-\omega}}{L_1^{y_t} - L_2^{y_t}} = \frac{b^{-\omega} - 1}{1 - b^{y_t}} L_1^{-y_t-\omega}, \qquad (3.5)$$

where $b \equiv L_2/L_1$. Moreover, the value of the cumulant $C_\times$ at the intersection approaches a *universal* value C_c in this limit.[3]

If one knew C_c in advance, then, for data in a given finite volume, a nice method for determining a nominal point of transition is to choose the r such that $C(r) = C_c$. The finite-size error in r_c caused by this procedure also scales as $L^{-y_t-\omega}$. This method is simpler and statistically a little cleaner than trying to find the intersection of two $C(r)$ curves for two different values of L. This is the method we shall use, but first we need a value of C_c. Because C_c is universal, its value can be measured from simulations of any model in the same universality class. We will use a value determined by Campostrini *et al.* [13], who also simulate a two-component lattice ϕ^4 theory. They obtained $C_c = 1.2430(1)(5)$, where the two numbers in parenthesis represent their statistical and systematic errors, respectively. In

---

[1]The value of roughly 1.5 comes from the scaling relationship $\nu = (2-\alpha)/d$ and the fact that the specific heat critical exponent α is very small in this universality class. The best value of α is $-0.01056(38)$ and comes from experiments in Earth orbit on superfluid ^{4}He [10,11]. (See in particular endnote 15 of Ref. [11], and see also footnote 2 of Ref. [13].) For comparison, theoretical values (making use of $\alpha = 2-d\nu$ as necessary) are $\alpha = -0.011(4)$, $-0.004(11)$, and $-0.0146(8)$ from three-dimensional (3D) series techniques [12], the ϵ expansion [12], and Monte Carlo [13].

[2]Values are $\omega = 0.789(11)$, $0.802(18)$, and $0.79(2)$ from 3D series techniques [12], the ϵ expansion [12], and Monte Carlo [14].

[3]For a nice numerical demonstration of this universality, see the Monte Carlo studies of Ising universality in Ref. [15].
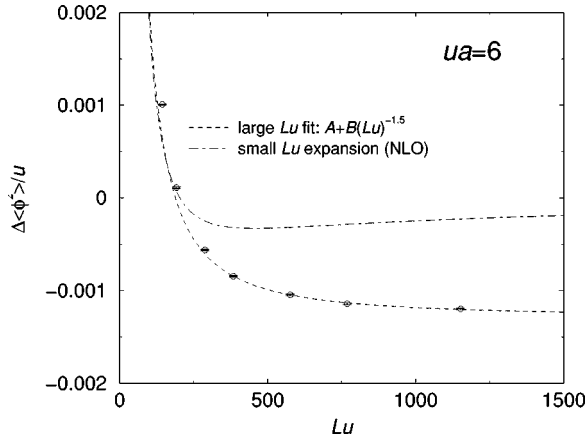
FIG. 2. Simulation results for $\Delta\langle\phi^2\rangle_c/u$ vs lattice size in physical units (Lu) for $ua=6$. The large Lu curve shown is a fit to the rightmost four data points, with confidence level 61%.

the rest of this paper, when quoting results for the transition in a given finite volume, we will mean the point where

$$C(r) = 1.243 \qquad (3.6)$$

for that volume. As a check, we have also made a much less accurate determination of C_c using our own simulations, which is discussed in Appendix D. We find $C_c = 1.240\,2(7)$, which we suspect has a systematic bias, discussed in the Appendix. The difference between these values of C_c is insignificant for our purposes. We have checked that the difference would only change our final results by a tiny fraction of an error bar.

IV. VOLUME DEPENDENCE OF $\Delta\langle\phi^2\rangle_c$

As discussed in the introduction, the only parameter of the continuum problem at the critical point is u. So the only length scale of the problem is $1/u$. The relevant measure of the size L of a finite-volume lattice relative to this scale is therefore Lu (and similarly the relevant measure of lattice spacing is ua). Figure 2 shows a plot of our results for $\Delta\langle\phi^2\rangle_c$ on $L\times L\times L$ lattices vs Lu for $ua=6$. As can be seen, our largest Lu values are clearly large: the data clearly shows nice convergence towards an infinite volume limit. To understand the size of the remaining finite-volume error, we will want to fit the volume dependence at large Lu to an appropriate scaling law.

A. Large volume scaling of $\Delta\langle\phi^2\rangle_c$

The scaling of large L corrections depends on universal critical exponents of the O(2) model, which is in the same universality class as the classical $N=2$ Heisenberg ferromagnet. The language of critical exponents in the O(2) model is borrowed from correspondence with the Heisenberg magnet, and $t \equiv r - r_c$ is referred to as the reduced "temperature" in this context, $C \propto d^2(\ln Z)/dt^2$ as the "specific heat," and so forth. It is important to emphasize that this language holds the potential for confusion because, in many applications (such as Bose-Einstein condensation at fixed density),

$t \equiv r - r_c$ is not, in fact, linearly related to the actual temperature of the system near the critical point, and $d^2(\ln Z)/dt^2$ is not directly the physical specific heat.[4] In any case, the analog of the "energy density" E/V under this correspondence is

$$\frac{E}{V} \propto \frac{d(\ln Z)}{Vdt} = \frac{1}{V}\frac{d}{dr}\ln\int[\mathcal{D}\phi]e^{-S[\phi]} \propto \langle\phi^2\rangle, \quad (4.1)$$

where $V=L^d$ is the system volume and $d=3$ is the dimension. The problem of understanding how the finite-volume corrections to $\langle\phi^2\rangle$ scale with L may therefore be stated in this language as the problem of how corrections to the "energy density" scale with L for anything in this universality class.

The standard finite-size scaling ansatz provided by renormalization group methods is that the free-energy density $f = -V^{-1}\ln Z$ scales as[5]

$$f(t,\{u_j\},L^{-1}) = f_{reg}(t,\{u_j\}) + b^{-d}f_{sing}(b^{y_t}t,\{u_jb^{y_j}\},b/L)$$
$$(4.2)$$

for periodic boundary conditions, where f_{reg} and f_{sing} generate the so-called regular and singular parts of the free energy in the infinite volume limit. (See Refs. [17,18] and references therein.) The length b is an arbitrary renormalization scale (block size), and $\{u_j\}$ denotes the set of infrared-irrelevant operators (with corresponding $y_j<0$). Standard notation for critical exponents is $\nu=1/y_t$, and we will denote the smallest $|y_j|$ associated with the irrelevant operators $\{u_j\}$ as ω.

Choosing $b=L$,

$$f(t,u_j,L^{-1}) = f_{reg}(t,u_j) + L^{-d}f_{sing}(L^{y_t}t,u_jL^{y_j},1).$$
$$(4.3)$$

The usual infinite-volume scaling form is obtained by taking $L\to\infty$ with t fixed, which, for the limit to exist, requires

$$f_{sing}(\tau,0,1) \sim \tau^{-d/y_t} \quad \text{as} \quad \tau\to\infty. \qquad (4.4)$$

In contrast, for fixed L, the free energy will be analytic in t, since there are no phase transitions in finite volume. We can make a Taylor expansion of the finite-volume free energy

---

[4] A uniform, nonrelativistic Bose gas is a constrained system: the particle density n is fixed. This constraint causes a different relationship of model parameters and the physical temperature than for unconstrained systems [16]. For example, the critical exponents $\tilde{x} = (\tilde\alpha, \tilde\beta, \tilde\gamma, \tilde\nu)$ of the actual system are related to the standard exponents $x = (\alpha, \beta, \gamma, \nu)$ of the field theory by (i) $\tilde\alpha = -\alpha/(1-\alpha)$, and $\tilde{x} = x/(1-\alpha)$ for the others, if $\alpha>0$, or (ii) $\tilde{x}=x$ if $\alpha<0$. This relation explains the difference between mean-field theory exponents for the O(2) model (e.g., $\alpha=1/2$) and the exponents of a noninteracting Bose gas (e.g., $\tilde\alpha=-1$).

[5] We have not included a "magnetic field" h coupling to ϕ, with a corresponding argument $b^{y_h}h$ in f_{sing}, because we will only be interested in the case $h=0$ and are not interested in correlations of ϕ (as opposed to ϕ^2), which could be generated by derivatives with respect to h.

(4.3) in t (as well as $\{u_j L^{y_j}\}$), which should be a useful expansion when the arguments of the scaling piece f_{sing} are small. That is, for situations where $L^{y_t} t \to 0$ as we take $L \to \infty$, we can Taylor expand Eq. (4.3) as

$$f = (A_0 + B_0 L^{-d} + C_0 L^{-d-\omega} + \cdots) + t(A_1 + B_1 L^{-d+y_t}$$
$$+ C_1 L^{-d+y_t-\omega} + \cdots) + t^2(A_2 + B_{20} L^{-d+2y_t} + \cdots)$$
$$+ \cdots, \qquad (4.5)$$

where we have only displayed the leading corrections due to irrelevant operators. Differentiating with respect to t to get the energy density, we find that $\langle \phi^2 \rangle$ scales in large volume as

$$\langle \phi^2 \rangle = (A_1 + B_1 L^{-d+y_t} + C_1 L^{-d+y_t-\omega} + \cdots)$$
$$+ 2t(A_2 + B_{20} L^{-d+2y_t} + \cdots) + \cdots. \qquad (4.6)$$

As mentioned earlier, use of the method of Binder cumulants to determine r_c means that, in our application,

$$t \sim L^{-y_t-\omega}. \qquad (4.7)$$

This indeed satisfies the condition $L^{y_t} t \to 0$ as $L \to \infty$, and so the expansion (4.6) is appropriate. For our application, we then have

$$\langle \phi^2 \rangle = A_1 + B_1 L^{-d+y_t} + A_2' L^{-y_t-\omega} + C_1' L^{-d+y_t-\omega} + \cdots. \qquad (4.8)$$

Using the standard scaling relation $\alpha = 2 - \nu d$ for the specific heat scaling exponent α, this may be rewritten in the form

$$\langle \phi^2 \rangle = A_1 + B_1 L^{-(1-\alpha)y_t} + A_2' L^{-y_t-\omega}$$
$$+ C_1' L^{-(1-\alpha)y_t-\omega} + \cdots. \qquad (4.9)$$

The value of α in the three-dimensional O(2) model is very small: $\alpha \simeq -0.013$, corresponding to the value $y_t \simeq 1.49$ quoted earlier [10–12,14].

The renormalizations Z_r and $\delta\phi^2$ that convert $\langle \phi^2 \rangle_{\text{lat}}$ into $\Delta\langle \phi^2 \rangle$ in Eq. (2.15) do not introduce any different powers of L, and so the form of the large-L expansion of $\Delta\langle \phi^2 \rangle$ is the same as that for $\langle \phi^2 \rangle$ in Eq. (4.9) above, though the coefficients are different.

B. Large-volume scaling for $\alpha=0$

Because we do not have large-volume data spanning many decades in L, α is zero for all practical purposes. And so one might as well use the $\alpha=0$ limit of the large-volume scaling (4.9), which corresponds to $y_t = d/2$. Typically, $\alpha = 0$ generates logarithms in a renormalization group analysis, which can appear as a superposition

$$\lim_{\alpha \to 0} \frac{s^{z+q\alpha} - s^z}{\alpha} = q s^z \ln s \qquad (4.10)$$

of power laws $s^{z+q\alpha}$ and s^z for some variable of interest s. One might therefore expect that the $\alpha \to 0$ limit of the large-volume scaling (4.9) is

$$\langle \phi^2 \rangle = A_1 + B_1 L^{-d/2} + L^{-d/2-\omega}(C \ln L + D) + \cdots. \qquad (4.11)$$

It is useful to verify the presence of a logarithm. If it were not there, we could include the first corrections to scaling in large L fits of our data using a three-parameter fit $[A_1, A_2, D]$ rather than a four-parameter fit $[A_1, B_1, C, D;$ or equivalently A_1, B_1, A_2', C_1' in Eq. (4.9)].

The existence of the logarithm may be directly related to the well-known logarithmic divergence of specific heat with t when $\alpha=0$. We give a renormalization group analysis in Appendix C that makes this explicit. Here, let us just note that the logarithm follows from an old proposal by Privman and Rudnick [19]. Ignore corrections to scaling for the moment, and suppose that at $\alpha=0$ the free energy had the general form (4.3) discussed earlier

$$f(t, L^{-1}) \sim f_{\text{reg}}(t) + L^{-d} f_{\text{sing}}(tL^{d/2}). \qquad (4.12)$$

In order to get a logarithmic divergence $\ln(t^{-1})$ of the specific heat in the infinite-volume limit, we need a term $t^2 \ln(t^{-1})$ in the free energy in that limit. So we must have

$$f_{\text{sing}}(\tau) \sim A\tau^2 \ln(\tau^{-1}) \quad \text{as} \quad \tau \to \infty. \qquad (4.13)$$

But this would give $f \sim f_{\text{reg}}(t) + At^2 \ln(t^{-1}L^{-d/2})$, which does not have a good $L \to \infty$ limit. The solution is to suppose that the $\alpha=0$ version of the free energy is instead

$$f(t, L^{-1}) \sim f_{\text{reg}}(t) + At^2 \ln(L^{d/2}) + L^{-d} f_{\text{sing}}(tL^{d/2}), \qquad (4.14)$$

which is what Privman and Rudnick proposed. Note that the term is analytic as $t \to 0$ for L fixed, as it must be. The term gives a $t \ln L$ contribution to the energy density E/V, which, for the $t \sim L^{-y_t-\omega}$ of interest to us, gives rise to the logarithm term in Eq. (4.11).

C. How large is large volume?

Before proceeding to numerical fits of the large-volume dependence, it is useful to first have an idea of how large L should be before one might reasonably hope for large-volume scaling to hold. From Fig. 2, we see that the finite-volume corrections to the continuum value of $\Delta\langle \phi^2 \rangle_c$ become 100% where the data crosses zero, at roughly $Lu \sim 200$. So, one might guess that this is very roughly the scale where scaling starts to set in—the scale that separates short-distance perturbative physics from long-distance critical-scaling physics. We can check this rough assessment from the other side. In the limit of small Lu, the physics of fluctuations is perturbative, and one may analytically compute the expected value of $\Delta\langle \phi^2 \rangle_c$ order by order in powers of Lu. We perform this computation in Appendix E in the continuum ($ua=0$) to next-to-leading order (NLO) in Lu, with the result that

$$\frac{\Delta\langle \phi^2 \rangle_c}{u} = \frac{6.440\,03}{(Lu)^{3/2}} - \frac{0.451\,570}{Lu} + O((Lu)^{-1/2}) \qquad (4.15)$$
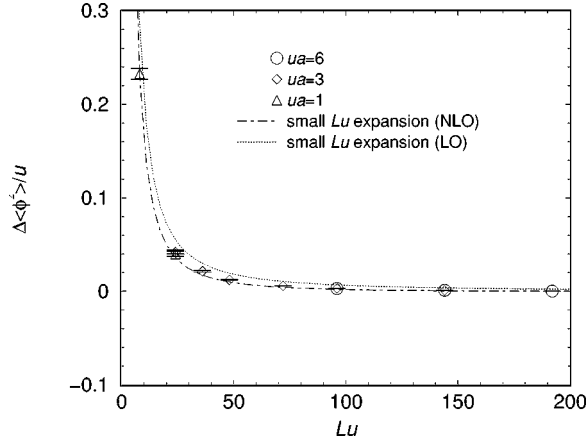
FIG. 3. Simulation results for $\Delta\langle\phi^2\rangle_c/u$ vs lattice size, showing more small volume data than Fig. 2. The dot-dash curve shows the next-to-leading-order small Lu expansion of Eq. (4.15). The dotted curve shows just the leading-order term of that expansion.

for our critical value (3.6) of the Binder cumulant. The resulting curve is shown in both Figs. 2 and 3 (as well as the leading-order small Lu result in Fig. 3). One can see that the small Lu expansion becomes unreliable past $Lu\sim200$, which is the same as the previous scale estimate. (There is obviously nothing precise about this statement. The scale at which the second term in the small Lu expansion becomes 50% of the first term, for example, is $Lu\sim50$.)

Interestingly, the scale $Lu\sim200$ is close to what one might estimate on the back of an envelope from a large-N approximation to the theory. In large N, one replaces the O(2) theory studied here by an O(N) theory of N scalar fields and solves the theory in the approximation that N is large—a program pursued for the problem of Bose-Einstein condensation of a nonrelativistic gas in Refs. [20,21]. In the $N\to\infty$ limit, one introduces an auxiliary field σ whose propagator represents a geometric sum of bubble diagrams, such as that shown in Fig. 4. The corresponding resummed propagator is proportional to

$$\frac{1}{\dfrac{3}{Nu}+\breve{\Sigma}_0(p)},\qquad(4.16)$$

where $\breve{\Sigma}_0(p)$ represents the basic massless bubble integral

$$\breve{\Sigma}_0(p)\equiv\frac{1}{2}\int_l\frac{1}{l^2|l+p|^2}=\frac{1}{16|p|}.\qquad(4.17)$$
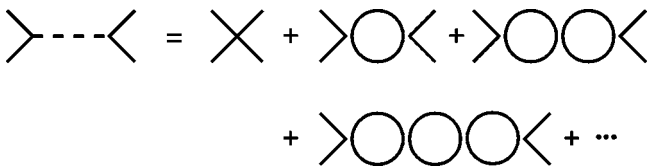

FIG. 4. Bubble chains, which are the source of scale dependence in large N calculations of $\Delta\langle\phi^2\rangle_c$ in O(N) theory [20,21].
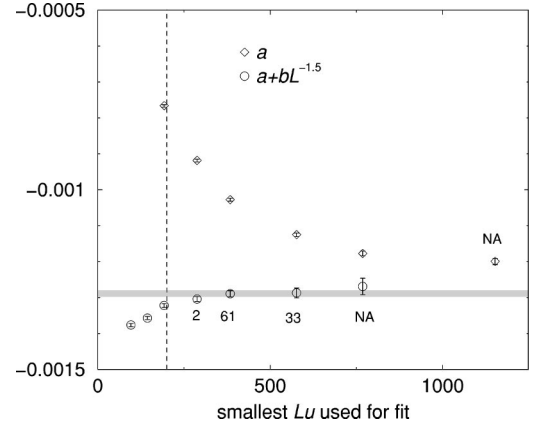

FIG. 5. Extrapolations of the $ua=6$ data of Fig. 2 to $L\to\infty$ under various assumptions of the functional form. The horizontal axis shows the smallest value of Lu of the data used for the fit. Percentage confidence levels are written next to each extrapolation whenever non-negligible ($\geq1\%$), and ``NA'' (not applicable) refers to those cases where the number of data points used for the fit equals the number of parameters.

The propagator (4.16) changes from its large momentum behavior ($\to$ constant) to its small momentum behavior ($\propto p$) at a scale given by $3/Nu\sim\Sigma_0(p)$. This corresponds to $p\sim Nu/48$ and so distance scales of order $L\sim2\pi/p\sim96\pi/Nu$. Setting $N=2$, we find $Lu\sim48\pi\sim150$. Of course, one would never hope that an estimation this crude would be useful beyond, at best, the factor of two level.

Our discussion of system size has implications for the validity of an early numerical study of the critical temperature for Bose-Einstein condensation for nonrelativistic gases [22]. We discuss this in Appendix F.

V. NUMERICAL EXTRAPOLATION OF $Lu\to\infty$

A. Extrapolating $\Delta\langle\phi^2\rangle_c$ to $Lu\to\infty$

We now examine fits of the $ua=6$ data of Fig. 2 to the large L scaling form of Eq. (4.11). The circles in Fig. 5 show the result of extrapolating to $L\to\infty$ using the leading-order scaling corrections in Eq. (4.11)—that is, ignoring the subleading terms, which involve the exponent ω. For comparison, the diamonds show what happens if we ignore finite-size effects altogether; the corresponding confidence levels are terrible. The vertical dashed line in the figure marks the moderate system size $L=200$ (discussed in the previous section), below which you should become suspicious of any attempt to fit the data to a large-volume scaling form.

A simple method for assigning a final result for the extrapolation is to take our best fit with a correct scaling form. As seen in Fig. 5, the leading-order scaling form $A+BL^{-d/2}$ is perfectly adequate for fitting our large Lu data. Our procedure is to fit the data for lattice sizes greater than or equal to a given $L_{\min}$, decreasing this minimum size for as long as the fit remains stable with a reasonable confidence level. We take as our estimate the 61% confidence level fit to $Lu\geq384$, which gives
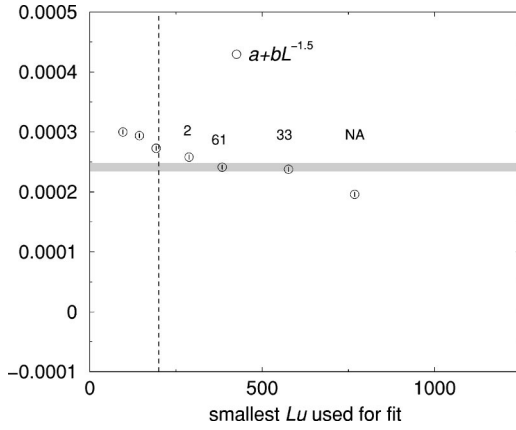
FIG. 6. As Fig. 5, but shows the magnitude of the finite-size correction to $\Delta\langle\phi^2\rangle_c/u$ at $Lu=576$, as determined by the fit.

$$\left[\frac{\Delta\langle\phi^2\rangle_c}{u}\right]_{ua=6} = -0.001\,289\,(9), \tag{5.1}$$

which is depicted by the shaded region of Fig. 5.

As described in Ref. [1], we will actually use $Lu=576$ as a reference point from which to derive finite volume and finite lattice-spacing corrections. Figure 6 is similar to Fig. 5 but shows the size of the finite-size correction at $Lu=576$, as determined by the fit. The best fit (the 61% confidence level one) gives

$$\left[\frac{\Delta\langle\phi^2\rangle_c}{u}\right]_{Lu=576} - \left[\frac{\Delta\langle\phi^2\rangle_c}{u}\right]_{Lu\to\infty} = 0.000\,241\,(7), \tag{5.2}$$

and we will use this difference, rather than the limit (5.1), in what follows. [The difference is determined by the coefficient B of our fit to $A+BL^{-d/2}$, and so is determined by all the data points of that fit; it is not simply our (Lu,ua) $=(576,6)$ data point minus the limit (5.1), which would produce a larger error.] As we shall see, $ua=6$ is a reasonably small value of ua, and we expect this to be a good estimate to the finite-volume corrections in the continuum ($ua\to 0$) limit.

As a check that corrections to scaling will not radically alter our results, we show as squares in Fig. 7 the result of fits to Eq. (4.11). The values are consistent with the previous result, with larger errors because we are fitting more parameters. The triangles show a simplified fit, with one less parameter, that ignores the logarithmic dependence.

B. Extrapolating r_c to $Lu\to\infty$

We will now make a similar analysis of finite-size effects for the critical value r_c of r. The continuum value of r is convention dependent—it depends on one's choice of renormalization scheme and renormalization scale. As discussed earlier, our convention will be to define r with $\overline{MS}$ regularization at the renormalization scale $\bar\mu=u/3$. The conversion formula (1.6) to other choices of $\bar\mu$ can be extracted from Eq. (2.13c) and the fact that the theory is super-renormalizable.
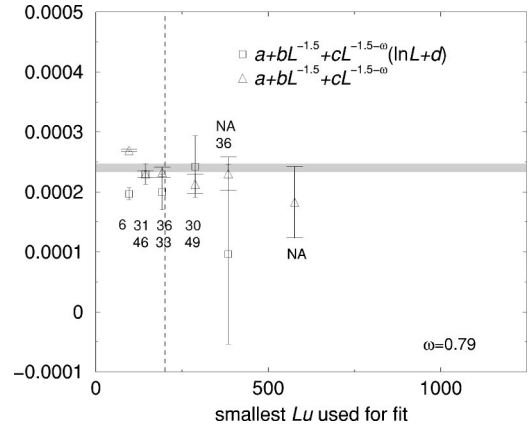

FIG. 7. As Fig. 6 but showing extrapolations that include corrections to scaling. Where two confidence levels are listed on top of each other, the upper one is for the square data point and the lower, for the triangular data point.

Figure 8 shows, for $ua=6$, the dependence on system size of our finite-volume determinations of $r_c(u/3)/u^2$. As discussed in Sec. III, the finite-size corrections are expected to scale as $L^{-y_t-\omega}$ as $L\to\infty$. Figure 9 shows the result of extrapolating an infinite-volume result by fitting various subsets of the data to $A+BL^{-(d/2)-\omega}$. Taking the highest confidence level fit,

$$\left[\frac{r_c(u/3)}{u^2}\right]_{ua=6} = 0.002\,882\,8\,(6). \tag{5.3}$$

Figure 10 shows the size of the finite-volume error at our canonical $Lu=576$, as determined by the fits,

$$\left[\frac{r_c(u/3)}{u^2}\right]_{Lu=576} - \left[\frac{r_c(u/3)}{u^2}\right]_{Lu=\infty} = -0.000\,006\,04(26). \tag{5.4}$$
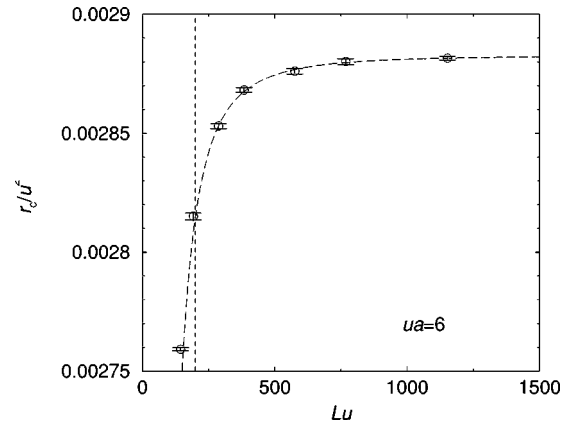

FIG. 8. $ua=6$ data for the nominal value of r_c/u^2 (defined in $\overline{MS}$ renormalization at renormalization scale $\bar\mu=u/3$) as a function of system size. The fit shown by the dashed line is the large-volume fit to all but the leftmost data point.
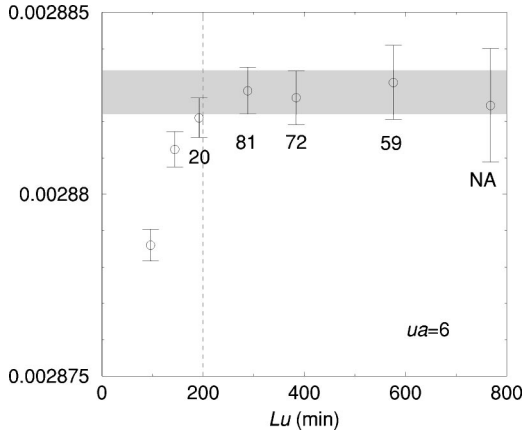
FIG. 9. Extrapolations of the $ua=6$ data of Fig. 8 to $L \to \infty$ using the functional form $A + BL^{-y_t - \omega}$. The horizontal axis shows the smallest value of Lu of the data used for the fit. Confidence levels are written as described for Fig. 5.

VI. NUMERICAL EXTRAPOLATION OF $ua \to 0$

A. Extrapolating $\Delta\langle\phi^2\rangle_c$ to $ua \to 0$

We will now discuss numerical results for the continuum limit $a \to 0$ while holding the physical volume of the lattice fixed. This can be expressed as $ua \to 0$ holding Lu fixed. Since the number $(L/a)^3$ of lattice sites we can practically include in a simulation is limited, we may obviously explore smaller values of ua when we fix smaller values of Lu. As a test that we understand our lattice-spacing errors, we have therefore made several simulations at the rather moderate system size of $Lu = 144$ (see the discussion of Sec. IV C). The results for the dependence of $\Delta\langle\phi^2\rangle_c/u$ on ua are shown by the squares in Fig. 11. If our corrections for $O(a)$ errors have been calculated correctly, the remaining error should be $O(a^2)$. Indeed, all but the largest two ua data points in Fig. 11 fit very well the functional form $A + B(ua)^2$, with a confidence level of 94%.

It is interesting to compare to what would have been obtained if we had used the same data but instead plotted the uncorrected
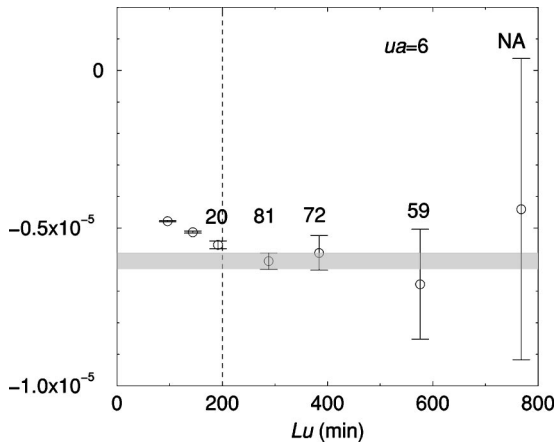

FIG. 10. As Fig. 9, but showing the magnitude of the finite-size correction to r_c/u^2 at $Lu = 576$.
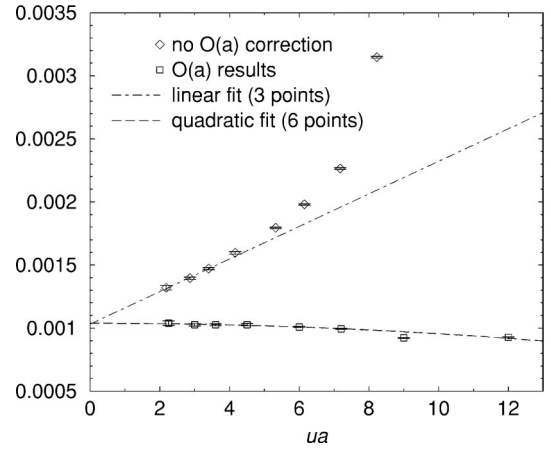

FIG. 11. The squares show results for $\Delta\langle\phi^2\rangle_c/u$ vs ua at $Lu = 144$. The line through them is a fit of the first six points to $A + B(ua)^2$. The diamonds represent the corresponding uncorrected data, as described in the text. To guide the eye, a straight line has been fit through the first three points, though the actual small ua behavior is linear×logarithmic.

$$\frac{\Delta\langle\Phi^2\rangle_c}{u_0} = \frac{1}{u_0}\left[\langle\Phi^2\rangle - \frac{\Sigma}{2\pi a}\right] \qquad (6.1)$$

vs $u_0 a$, where Φ and u_0 are the bare lattice fields and coupling of Eq. (2.1). This uncorrected data is represented by the diamonds in Fig. 11. One clearly sees the $O(a)$ corrections. We should make clear that this is still $Lu = 144$ data and is not $Lu_0 = 144$ data, which would have required additional simulations.

Figure 12 shows the ua dependence at a reasonably large physical system size of $Lu = 576$. We show extrapolations of the $ua \to 0$ limit in Fig. 13. Here, the 10% confidence levels of fits to $A + B(ua)^2$ are less spectacular than the $Lu = 144$ data, though not unreasonable. Because of the lower confidence levels, we have been a little more conservative in our error estimate. We take as our result for the $ua \to 0$ limit the shaded region of Fig. 13, which has been chosen to cover both the 10–15% confidence level fits:
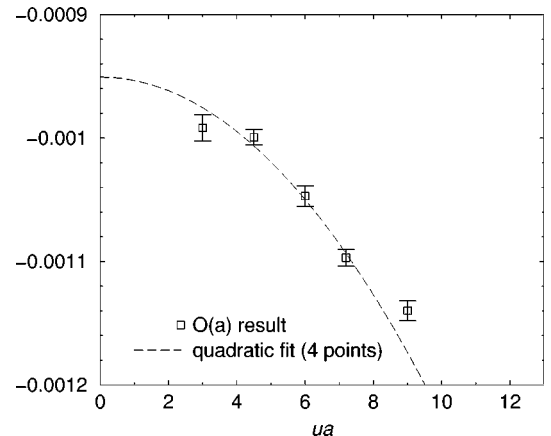

FIG. 12. Results for $\Delta\langle\phi^2\rangle_c/u$ vs ua at $Lu = 576$. The line is a fit of $A + B(ua)^2$ to all but the rightmost data point.
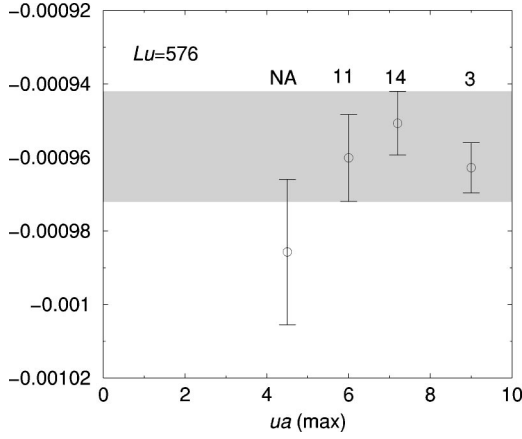
FIG. 13. Extrapolations of the data of Fig. 12 to $ua=0$ fitting to the form $A+B(ua)^2$. The horizontal axis shows the maximum value of ua used for each fit. Confidence levels are written as described for Fig. 5.

$$\left[\frac{\Delta\langle\phi^2\rangle_c}{u^2}\right]_{Lu=576} = -0.000\,957\,(15). \qquad (6.2)$$

Combining this with the finite-volume correction (5.2), and adding errors in quadrature, we arrive at our final value (1.4) for the infinite-volume continuum limit. Note that the dominant error in this estimate comes from the $ua \to 0$ extrapolation.

B. Extrapolating r_c to $ua \to 0$

The circles in Fig. 14 show the dependence of r_c on ua at the medium system size of $Lu=144$, where we may simulate down to relatively small values of ua. The data fits well to a linear dependence on ua, with the fit shown to the first six points in the figure having a 38% confidence level. The triangles in the same figure show similar dependence for the reasonably large system size of $Lu=576$. The corresponding extrapolations to $ua=0$ based on linear fits are shown in Fig. 15. We take the $ua=0$ extrapolation to be
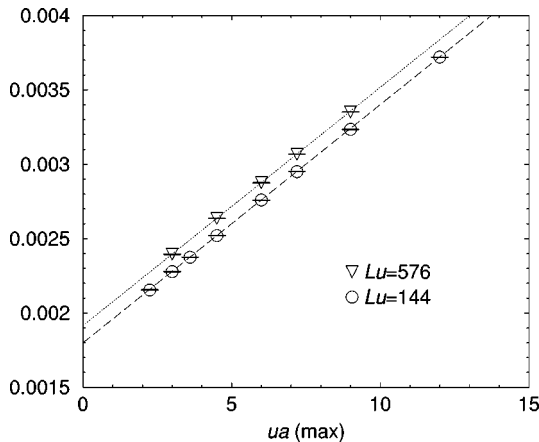

FIG. 14. Results for r_c/u^2 vs ua at $Lu=144$ and $Lu=576$ (defined in $\overline{\text{MS}}$ renormalization at renormalization scale $\bar{\mu}=u/3$). The lines are linear fits.
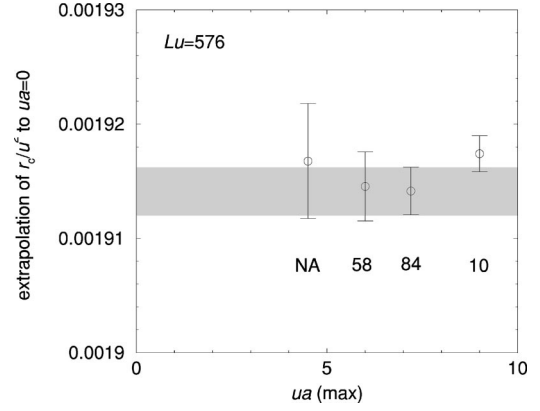

FIG. 15. Linear extrapolations of the $Lu=576$ data of Fig. 14 to $ua=0$. The horizontal axis shows the maximum value of ua used for each fit. Confidence levels are written as described for Fig. 5.

$$\left[\frac{r_c(u/3)}{u^2}\right]_{Lu=576} = 0.001\,914\,1\,(21), \qquad (6.3)$$

as shown by the shaded region of the figure. Combining with our estimate (5.4) of the finite-size error at $Lu=576$ gives our final result (1.5) for the infinite-volume continuum limit. Again, the dominant error comes from the $ua \to 0$ extrapolation.

C. Interdependence of $Lu \to \infty$ and $ua \to 0$ extrapolations

In this paper, we have treated the extrapolation of our finite-volume correction, taken from $ua=6$ data, as independent from our continuum extrapolation, taken from $Lu=576$ data. Consider the case of $\Delta\langle\phi^2\rangle_c/u$. In principle, the two extrapolations are not completely independent because the coefficient B in the form $A+BL^{-d/2}$ used for our large L extrapolation is not universal. Its value will have some dependence on ua. For our procedure, we would like to know the value of B at $ua=0$, to obtain the large L correction (5.2) at $ua=0$. Instead, we have the large L correction at $ua=6$, which will be slightly different. In numerical terms, we will have underestimated our systematic error if $B[ua=6]$ differs from $B[ua=0]$ by $\sim 7\%$, which is the final error on $\Delta\langle\phi^2\rangle_c/u$ quoted in Eq. (1.4) relative to the size of the finite-volume correction (5.2).

How does the coefficient B depend on ua as $ua \to 0$? Because of our improvements to the action and to the operator ϕ^2, the answer is that small ua corrections to B vanish as $(ua)^3$. To see this, note that the only quantities we have *not* matched through $O[(ua)^2]$ are r and $\delta\phi^2$. However, neither of these contribute to B. $\delta\phi^2$ is a constant and therefore Lu independent, and our procedure tunes to the critical value of (the continuum parameter) r whether or not the lattice parameter is correctly matched to the continuum one. The residual difference between lattice and continuum r does appear in Eq. (2.16), but, because $r-r_c$ vanishes as $L^{-\omega-d/2}$, this does not contribute to B either. We should not expect such a high-order correction to be of any consequence.

There is an alternate way of fitting our data that makes it easier to check this. We can fit all data at large Lu and relatively small ua to a form that allows both spacing and volume dependence,

$$\frac{\Delta\langle\phi^2\rangle_c}{u} = A + B(Lu)^{-y_t} + C(ua)^2. \qquad (6.4)$$

Based on our fits at fixed Lu and fixed ua, we expect this form is sufficient if we use only data with $Lu \geqslant 384$ and $ua \leqslant 8$. Fitting all such data gives $\Delta\langle\phi^2\rangle_c/u = -0.001\,194\,(8)$ with $\chi^2/(\text{degrees of freedom}) = 15.3/8$ (5% confidence level). The result is consistent with our quoted result, and has smaller errors. The quality of the fit is not very good, which is why we quote the larger error bars of our other analysis. However, adding a term that allows B to vary with ua (that is, a ua and Lu dependent term) does not improve the quality of the fit. Adding the term $D(Lu)^{-y_t}(ua)^m$ and doing a four parameter fit changes χ^2 by less than 1 for $m=2$ or $m=3$; so the data show no evidence that such a term is large enough to be important.

We do not understand why the fit to all data has such a large χ^2 [$\chi^2/(\text{degrees of freedom}) = 15.3/8$]. The three lowest ua data points are the main outliers; the two $ua=3$ points are each at 2σ. However, the $(Lu,ua) = (384,3)$ point is off in the opposite direction as the $(Lu,ua) = (576,3)$ and $(Lu,ua) = (384,4)$ points, so there is no systematic trend in the residuals and we have no reason to believe that some additional lattice-spacing or volume-dependent term is missing in our fitting procedure.

Finally, there is a minor, independent issue in our main analysis. The statistical part of our errors in our original infinite volume and continuum extrapolations are correlated, since both of these extrapolations included the $(Lu,ua) = (576,6)$ data point. However, since the error from the continuum extrapolation dominated that from the infinite-volume extrapolation, any statistical cross correlation between those errors will not have a significant effect.

APPENDIX A: TABULATED DATA

To give a rough idea of the size of our data sets, we have listed in Table I a nominal decorrelation time τ for each simulation, along with the amount of data we have in units of 2τ. In our convention, $\tau=0.5$ represents completely uncorrelated data. Our decorrelation times are in units of sweeps, where one "sweep" consists of both a heatbath sweep and a multi-grid update. More than one time is shown in cases where simulations were made at different values of r (before reweighting).

Our nominal decorrelation time is the largest integrated decorrelation time of the various expectations required in the computation of the Binder cumulant and of $\langle\phi^2\rangle$. These include the integrated decorrelation times associated with measurements of P, $P\phi^2$, $P\bar{\phi}^2$, and $P\bar{\phi}^4$ (and also times associated with cross correlations between these), where

$$P \equiv \exp\left(-\frac{1}{2} V \delta r \overline{\phi^2}\right) \qquad (A1)$$

is the canonical reweighting factor, as in Eq. (2.22). We found in all cases that the longest decorrelation time was that associated with $\bar{\phi}^2$. The integrated decorrelation time for a single operator is given by

$$\tau \equiv \frac{1}{2} + \sum_{n=1}^{\infty} \frac{C(n)}{C(0)}, \qquad (A2)$$

where

$$C(n) = \frac{1}{(N-n)} \sum_{i=1}^{N-n} O_i O_{i+n} - \left(\frac{1}{N}\sum_{i=1}^{N} O_i\right)^2, \qquad (A3)$$

is the autocorrelation function associated with the desired operator O. In practice, the sum in Eq. (A2) must be cut off because of degrading statistics, and we cut it off when $C(n)/C(0)$ first drops below 0.05.

APPENDIX B: MATCHING CONTINUUM AND LATTICE THEORIES

1. General discussion

In this appendix, we discuss the $O(a)$ and $O(a^2)$ improvement of three-dimensional scalar field theory on the lattice. For the sake of generality, and because it is not any harder, we will discuss $O(N)$ scalar field theory of N real fields $\phi = (\phi_1, \phi_2, \ldots, \phi_N)$. The case of interest to the present paper is $N=2$. As in Eq. (2.12), the lattice Lagrangian is defined to be

$$\mathcal{L} = a^3 \sum_{\mathbf{x}} \left[\frac{Z_\phi}{2} \sum_{i=1}^{N} (-\phi_i \mathbf{\nabla}_{\text{lat}}^2 \phi_i) + \frac{Z_r(r+\delta r)}{2}\phi^2 \right.$$
$$\left. + \frac{u+\delta u}{4!}(\phi^2)^2 \right], \qquad (B1)$$

where

$$\phi^2 \equiv \sum_{i=1}^{N} \phi_i^2, \qquad (B2)$$

and ϕ, r, and u are just the (UV renormalized) continuum fields and parameters in lattice units. So, $\phi_{\text{lat}} = a^{1/2}\phi_{\text{cont}}$, $u_{\text{lat}} = a u_{\text{cont}}$, and $r_{\text{lat}} = a^2 r_{\text{cont}}$. Of these, r_{cont} is the only continuum parameter that requires UV renormalization and should be understood as renormalized with dimensional regularization and the $\overline{\text{MS}}$ scheme. In this appendix, we will calculate, to a given order in lattice spacing, the necessary

TABLE I. All analysis data, including nominal decorrelation time τ.

Lu	ua	L/a	$\Delta\langle\phi^2\rangle_{\rm c}/u$	$r_{\rm c}/u^2$	$\tau_{\rm decorr}$	$N_{\rm sweeps}/2\tau$
8	1	8	0.2325(58)	$-0.02992(98)$	0.6	16868
24	1	24	0.0400(28)	$-0.00207(37)$	0.5	1070
24	3	8	0.0420(21)	$-0.00249(26)$	0.5	11470
36	3	12	0.02164(96)	0.00027(13)	0.5	38070
48	3	16	0.012322(95)	0.001233(12)	0.6	231566
72	3	24	0.00575(15)	0.001906(25)	0.7	9993
96	3	32	0.003212(65)	0.0021036(79)	0.8	26406
96	6	16	0.0030836(86)	0.0025981(12)	0.8	1235650
144	2.25	64	0.001039(18)	0.0021542(24)	1.3	205420
144	3	48	0.0010254(98)	0.0022783(16)	1.4	158458
144	3.6	40	0.0010253(83)	0.00237477(99)	1.1	373163
144	4.5	32	0.0010267(97)	0.0025199(13)	1.2	370142
144	6	24	0.0010083(44)	0.00275922(62)	1.1	940826
144	7.2	20	0.0009940(40)	0.00295088(70)	1.0	863928
144	9	16	0.0009222(43)	0.00323454(58)	1.1	1213680
144	12	12	0.0009256(43)	0.00372103(51)	0.7	1844310
192	6	32	0.0001118(88)	0.0028151(14)	1.7	192227
288	3	96	$-0.0004299(90)$	0.0023640(13)	5.7	21604
288	6	48	$-0.0005625(76)$	0.0028531(10)	3.4	50516
384	3	128	$-0.0007484(57)$	0.00238397(94)	3.7/5.7	69038
384	4	96	$-0.000799(11)$	0.0025498(15)	7.4	12316
384	4.8	80	$-0.0008055(80)$	0.0026760(14)	6.3	18797
384	6	64	$-0.0008455(71)$	0.0028682(10)	5.7	14591
384	8	48	$-0.0009131(78)$	0.0031875(12)	3.7	20958
384	12	32	$-0.01217(18)$	0.0038358(19)	3.6	6021
576	3	192	$-0.000992(11)$	0.0023957(16)	17.5/8.5	4458
576	4.5	128	$-0.0009993(64)$	0.00263522(80)	12.5	12212
576	6	96	$-0.0010470(83)$	0.0028761(11)	7.4/7.9	7196
576	7.2	80	$-0.0010968(68)$	0.00306843(97)	10.8/6.2	13493
576	9	64	$-0.0011398(80)$	0.0033525(11)	10.5	4007
768	6	128	$-0.001142(11)$	0.0028802(13)	14.3/13.1	3074
1152	6	192	$-0.0011999(86)$	0.00288154(80)	7.4/18.5/10.1	6342

counter-terms Z_ϕ, Z_r, δr, and δu required to implement this correspondence between continuum and lattice variables. To match the lattice and continuum theories to high orders in a, we would need to include other operators in our lattice theory, such as ϕ^6, $\phi^2|\nabla\phi|^2$, and so forth. However, these will turn out to be unnecessary at the order to which we will work.

A given local lattice action will never perfectly reproduce the continuum action. For small ua, the error in how a given lattice action treats physics at the distance scale a may be computed and compensated for by perturbative calculations. The discrepancy in how a given lattice action, with given parameters, treats the nonperturbative physics at the distance scale $1/u$ cannot. It is therefore important that the lattice action be close enough to the continuum action that errors at the scale $1/u$ are higher order in a than whatever is desired. In order to improve our simulations and measurement of $\Delta\langle\phi^2\rangle_{\rm c}$ to $O(a)$ accuracy, it is necessary to (a) match the lattice action and parameters so that, at the scale $1/u$, it reproduces the physics of the continuum action up to and including $O(a)$; and (b) match the lattice and continuum defi-

nitions of the operator ϕ^2 to the same order, so that the measurements of $\Delta\langle\phi^2\rangle_{\rm c}$ will match up. Actually, the first requirement is slightly overstated. To measure $\Delta\langle\phi^2\rangle_{\rm c}$ to $O(a)$, it is not necessary to match the lattice and continuum parameters r to that order. That is because, in the simulations, we will simply vary the coefficient of ϕ^2 in the action until we find the transition—we do not need to know its relation to $r_{\rm cont}$ to do this.

In this appendix, we will match $r_{\rm cont}$ to the lattice just to $O(a^0)$. This will make possible a determination of the continuum value of the critical value $r_{\rm c}$, but $O(a)$ errors will remain and must be removed by extrapolation to the continuum limit. We will match the continuum and lattice definitions of the operator ϕ^2 through $O(a)$, so that we can make an $O(a)$ improved calculation of $\langle\phi^2\rangle_{\rm c}$. We will also match the lattice action through $O(a^2)$ [except for the matching of r just discussed], rather than simply $O(a)$, because it is not that difficult [compared to the $O(a)$ matching of ϕ^2] and should improve the ua dependence of infinite-volume extrapolations of our data, as discussed in Sec. VI C.
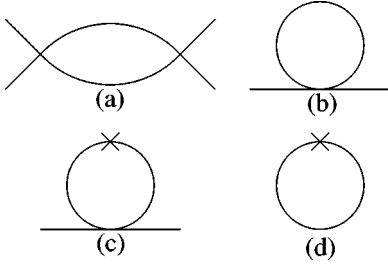
FIG. 16. The one-loop graphs needed for the renormalization. A cross represents a ϕ^2 insertion, which in turn could represent either (i) a perturbative insertion of the $r\phi^2$ term of the action or (ii) the ϕ^2 operator associated with calculating the expectation $\langle\phi^2\rangle$.

At tree level, the infrared behavior of the lattice and continuum theories are the same up to corrections suppressed by at least a^2; the power of a may be higher if we choose the lattice ∇^2 appropriately. However, there are ''radiative'' corrections induced in the infrared (IR) physics by the nonlinearity of the theory, together with the UV difference between the lattice and continuum theories. The diagrams of Fig. 16, for instance, differ on the lattice from their continuum values because the dispersion relations of the scalar fields differ in the UV, and the loop momentum integration integrates over this region. These effects are suppressed by powers of the couplings; the radiative correction to the scalar four-point function, for instance, clearly depends on u^2. On dimensional grounds, the difference between lattice and continuum values of this diagram must go as u^2a, so these diagrams lead to $O(a)$ differences between the lattice and continuum theories. The difference between lattice and continuum values of these diagrams may be removed by a renormalization of the parameters of the lattice theory.

As discussed in the main text, we will be interested not only in how to renormalize the parameters of the action but also in how to translate expectation values of the operator ϕ^2 between the lattice and continuum. It will be convenient to talk directly about the operator ϕ^2, which is associated with UV divergences in the continuum, rather than $\Delta\langle\phi^2\rangle$, which is not. We will define ϕ^2 in the continuum also using $\overline{\text{MS}}$ renormalization. In general, operators with the same symmetry can mix under renormalization, and the lattice operator ϕ^2 will correspond to some superposition of the unit continuum operator, the renormalized ϕ^2 continuum operator, and higher-dimensional renormalized continuum operators such as ϕ^4:

$$a^{-1}(\phi^2)_{\text{lat}} = c_0 + c_2(\phi^2)_{\text{cont}} + c_4(\phi^4)_{\text{cont}} + \cdots. \quad \text{(B3)}$$

However, our particular interest is in expectation values at the transition. For this application, the effects of higher-and-higher-dimensional operators on the right-hand side of Eq. (B3) become suppressed by more and more powers of ua. For example, c_2 is O(1), and the expectation value of the renormalized continuum operator ϕ^2 is, by dimensional analysis, $O(u)$ at the transition. So, the $c_2(\phi^2)_{\text{cont}}$ term contributes $O(u)$ to the expectation. In contrast, the lowest-order diagram that contributes to mixing between ϕ^2 and ϕ^4 is shown in Fig. 17 and gives $c_4 = O(u^2a^3)$, where the u^2
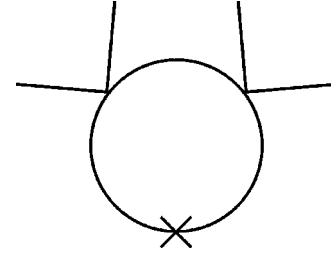

FIG. 17. A diagram contributing to the mixing of the ϕ^2 and ϕ^4 operators.

counts the two vertices in Fig. 17 and the a^3 then follows by dimensional analysis. But, also by dimensional analysis, the renormalized continuum expectation $\langle\phi^4\rangle$ is $O(u^2)$. So, the $c_4(\phi^4)_{\text{cont}}$ term contributes $O(u^4a^3)$ to the expectation, down by three powers of ua from $c_2(\phi^2)_{\text{cont}}$. Our goal will be to compute the $O(a)$ corrections to $\Delta\langle\phi^2\rangle_c$, for which it is therefore adequate to compute just c_0 and c_2 above.

The diagrams that contribute to c_2 are the same as those that contribute to the multiplicative renormalization of the coefficient r of ϕ^2 in the action, and $1/c_2$ is the same as the Z_r introduced previously. Rearranging the terms in Eq. (B3), we will write

$$a(\phi^2)_{\text{cont}} = Z_r(\phi^2)_{\text{lat}} - \delta\phi^2 + O((ua)^4), \quad \text{(B4)}$$

where $\delta\phi^2$ represents a c-number (ac_0/c_2) parametrizing mixing with the unit operator, which we shall calculate.

We will see later that, for the purpose of calculating the $O(a)$ corrections to $\Delta\langle\phi^2\rangle_c$, all that is strictly required is one-loop results for Z_ϕ, Z_r, δu, and δr, and three-loop results for $\delta\phi^2$. To determine r_c [just at $O(a^0)$] requires tree results for Z_ϕ, δu, and Z_r, and two-loop results for δr. If one made a three-loop computation of δr (which we have not), one could obtain the $O(a)$ corrections for r_c as well. To match the action through $O(a^2)$, except for r, one wants a two-loop determination of Z_ϕ and δu. As discussed in Sec. VI C, it will also be useful to have a two-loop result for Z_r.

Now we turn to the calculations. For the remainder of this appendix, we will work exclusively in lattice units ($a=1$).

2. One-loop results

A one-loop renormalization calculation will determine the $O(a)$ contributions to the quantities Z_ϕ, δu, and Z_r, and will find the $O(1/a)$ contributions to δm^2 and $\delta\langle\phi^2\rangle$. The details of the power counting used here may be found in [23]. In the small lattice-spacing limit, the momentum scale $r^{1/2}$ associated with the parameter r is small compared to the scale $1/a$ where the lattice and continuum theories differ. So, for the specific purpose of a calculation to match the lattice and continuum theories, the $r\phi^2$ term in the action (as well as the $u\phi^4$ term) may be treated perturbatively.

The required graphs are shown in Fig. 16. Evaluating the graphs requires choosing a lattice Laplacian, and for completeness we will consider both the unimproved Eq. (2.2) and improved Eq. (2.3) choices described in the main text. The evaluation of the one-loop graphs requires two integrals

$$\frac{\Sigma}{4\pi} \equiv \int_{\text{BZ}(2\pi)^3} \frac{d^3k}{\tilde{k}^2}, \tag{B5}$$

$$\frac{\xi}{4\pi} \equiv \int_{\text{BZ}} \frac{d^3k}{(2\pi)^3} \frac{1}{(\tilde{k}^2)^2} - \int_{\mathbb{R}^3} \frac{d^3k}{(2\pi)^3} \frac{1}{k^4}. \tag{B6}$$

Here, we use the shorthand BZ to mean k lies within the Brillouin zone, meaning each $k_i \in [-\pi, \pi]$. The notation $\tilde{k}^2$ is introduced in Eq. (2.4). The integrals that determine ξ are each IR singular and some regulation is implied, for instance adding m^2 to both k^2 and $\tilde{k}^2$ and taking the limit as $m^2 \to 0$. The numerical values of the integrals, accurate to ± 1 in the last digit, are[6]

$$\Sigma_{\text{U}} = 3.175\,911\,535\,625\,22, \quad \Sigma_{\text{I}} = 2.752\,383\,911\,307\,52,$$

$$\xi_{\text{U}} = 0.152\,859\,324\,966\,101, \quad \xi_{\text{I}} = -0.083\,647\,053\,040\,968. \tag{B7}$$

Note that the sign of ξ depends on whether we use an improved lattice Laplacian. This is possible because ξ represents the difference of a graph between lattice and continuum theories. The lattice contribution is larger inside the Brillouin zone, but the continuum integral receives contributions from outside the zone as well; the sign depends on which effect is larger.

At one loop, the renormalizations are (in lattice units)

$$\delta u_{1l} = \frac{(N+8)}{6} \frac{\xi}{4\pi} u^2, \tag{B8}$$

$$Z_{\phi,1l} - 1 = 0, \tag{B9}$$

$$Z_{r,1l} - 1 = \frac{(N+2)}{6} \frac{\xi}{4\pi} u, \tag{B10}$$

$$\delta r_{1l} = -\frac{(N+2)}{6} \frac{\Sigma}{4\pi}, \tag{B11}$$

$$\delta\phi_{1l}^2 = N \frac{\Sigma}{4\pi}. \tag{B12}$$

3. Two-loop results

For the renormalizations Z_ϕ and Z_r, it makes no sense to carry the renormalization to two loops unless we use the improved lattice Laplacian, because already at tree level, the unimproved Laplacian gives $O(a^2)$ level errors in the propagator. The two-loop results require several more graphs as well as the inclusion in one-loop graphs of one-loop mass and coupling counterterms. (See Fig. 18.) Four more inte-
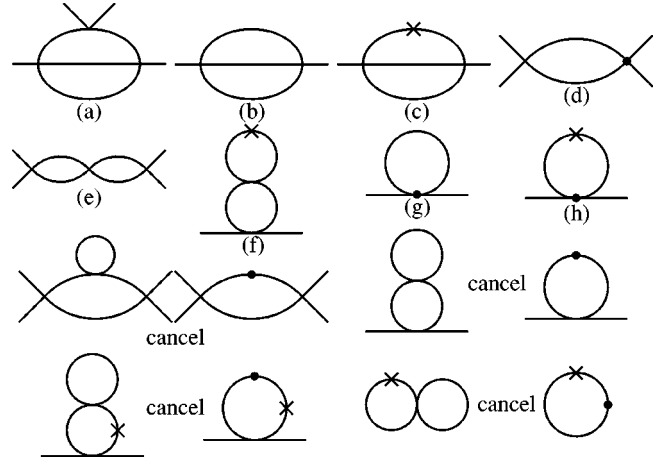

FIG. 18. All required two-loop graphs and one-loop graphs with one-loop counterterm insertions, shown as heavy dots on lines (mass counterterms) or at vertices (coupling counterterms). The last eight graphs cancel in pairs. Diagrams (a), (d), and (e) are not separately IR convergent; diagram (d) must be distributed between the other two to produce IR convergent integrals.

grals are needed, which we will evaluate in a moment. The complete two-loop result for general N is

$$\delta u_{2l} - \delta u_{1l} = \left[\frac{(N^2 + 6N + 20)}{36} \left(\frac{\xi}{4\pi} \right)^2 - \frac{(5N + 22)}{9} \frac{C_1}{(4\pi)^2} \right] u^3, \tag{B13}$$

$$Z_{\phi,2l} - 1 = \frac{(N+2)}{18} \frac{C_2}{(4\pi)^2} u^2, \tag{B14}$$

$$Z_{r,2l} - Z_{r,1l} = \left[\left(\frac{N+2}{6} \right)^2 \left(\frac{\xi}{4\pi} \right)^2 - \frac{(N+2)}{6} \frac{C_1}{(4\pi)^2} \right] u^2, \tag{B15}$$

$$\delta r_{2l} - \delta r_{1l} = \frac{(N+2)}{18(4\pi)^2} \left[C_3 + \ln\left(\frac{6}{\mu} \right) - 3\Sigma\xi \right] u^2, \tag{B16}$$

$$\delta\phi_{2l}^2 - \delta\phi_{1l}^2 = \frac{N(N+2)}{6} \frac{\Sigma\xi}{(4\pi)^2} u. \tag{B17}$$

The three numerical constants C_1, C_2, and C_3 are given for the improved Laplacian in Eq. (2.14). Only C_3 can be usefully defined for the unimproved case,[7] where it is $C_{3,\text{U}} = 0.088\,480\,10$.

Now, we detail the calculation of the constants C_1 through C_3. We will use the following shorthands: $\int_{k,\text{BZ}}$ means $\int d^3k/(2\pi)^3$, with range the Brillouin zone $[-\pi, \pi]^3$; whereas $\int_{k,\mathbb{R}^3}$ is the same but integrated over all 3-space. Further, we define the following integrals, which will come up repeatedly:

---

[6]An analytic result [6] for Σ_{U} is $8/\pi(18 + 12\sqrt{2} - 10\sqrt{3} - 7\sqrt{6})[K((2-\sqrt{3})^2(\sqrt{3}-\sqrt{2})^2)]^2$, where $K(k) = F(\frac{\pi}{2}, k)$ is the complete elliptic integral of the first kind.

[7]In Ref. [24], this constant is called ζ.

$$I_{\mathrm{L}}(p) = \int_{q,\mathrm{BZ}} \frac{1}{\widetilde{q}^2(\widetilde{p+q})^2}, \qquad (B18)$$

$$I_{\mathrm{C}}(p) = \int_{q,\mathbb{R}^3} \frac{1}{q^2(p+q)^2} = \frac{1}{8|p|}. \qquad (B19)$$

We begin with the two-loop vertex correction, graph (a) of Fig. 18. The required integral, including the appropriate amount of the one-loop counterterm graph (d), is

$$\frac{C_1}{(4\pi)^2} = \int_{k,\mathrm{BZ}} \frac{1}{(\widetilde{k}^2)^2}\left\{ I_{\mathrm{L}}(k) - \frac{\xi}{4\pi}\right\} - \int_{k,\mathbb{R}^3} \frac{1}{k^4} I_{\mathrm{C}}(k). \qquad (B20)$$

We rearrange the original integral into three parts,

$$\int_{k,\mathrm{BZ}} \frac{1}{(\widetilde{k}^2)^2}\left\{ I_{\mathrm{L}}(k) - \frac{1}{8k} - \frac{\xi}{4\pi}\right\} + \int_{k,\mathrm{BZ}} \frac{1}{8k}\left(\frac{1}{(\widetilde{k}^2)^2} - \frac{1}{k^4}\right)$$

$$- \int_{k,\mathbb{R}^3-\mathrm{BZ}}\left(\frac{1}{8k^5}\right). \qquad (B21)$$

All three of the above integrals are convergent, provided we use the improved Laplacian. The first integral is IR well behaved because the two counterterms cancel $I_{\mathrm{L}}(k)$ up to a k^2 correction, which in the small k limit is $I_{\mathrm{L}}(k) - (1/8k) - (\xi/4\pi) \to (0.012\,543\,8)k^2/4\pi$.

To get accurate numerical answers, we perform all 3D integrals by quadratures. Dealing with the double poles that appear in I_{L} is touchy, and requires adaptive mesh refinement techniques. We improve the precision of each final result by repeating the full integration at several spacings and extrapolating (Richardson extrapolation). The first integral in Eq. (B21) gives $(0.036\,000\,3)/16\pi^2$, and the second gives $(0.054\,568\,958)/16\pi^2$. The last integral, over $\mathbb{R}^3-\mathrm{BZ}$, may be rearranged into

$$- \frac{3}{16\pi^5}\int_0^1 dx \int_0^1 dy \frac{1}{(1+x^2+y^2)^{5/2}}, \qquad (B22)$$

which gives $-(0.035\,507\,296\,027\cdots)/16\pi^2$. These sum to give $C_1 = 0.055\,061\,2$.

Besides this graph, there is graph (e), which gives

$$\left(\int_{k,\mathrm{BZ}} \frac{1}{(\widetilde{k}^2)^2}\right)^2 - \left(\int_{k,\mathbb{R}^3} \frac{1}{k^4}\right)^2, \qquad (B23)$$

which is *not* IR convergent. However, including -2 times the counterterm diagram (d),

$$-2\left(\int_{k,\mathrm{BZ}} \frac{1}{(\widetilde{k}^2)^2}\right)\left(\int_{k,\mathrm{BZ}} \frac{1}{(\widetilde{k}^2)^2} - \int_{k,\mathbb{R}^3} \frac{1}{k^4}\right), \qquad (B24)$$

gives $-(\xi/4\pi)^2$. No new integrals are required. It is a nontrivial check on the calculation that the sum of the coefficients arising from diagrams (a) and (e) precisely absorb diagram (d).

The next integral is the $O(p^2)$ contribution from the setting sun diagram (b),

$$\frac{C_2}{(4\pi)^2} = \lim_{p\to 0} \frac{1}{p^2}\left\{ \int_{k,\mathrm{BZ}}\left(\frac{1}{(\widetilde{k+p})^2} - \frac{1}{\widetilde{k}^2}\right) I_{\mathrm{L}}(k)\right.$$

$$\left. - \int_{k,\mathbb{R}^3}\left(\frac{1}{(k+p)^2} - \frac{1}{k^2}\right) I_{\mathrm{C}}(k)\right\}. \qquad (B25)$$

The first trick is to note that

$$\int_{k,\mathrm{BZ}}\left(\frac{1}{(\widetilde{k+p})^2} - \frac{1}{\widetilde{k}^2}\right) = 0, \qquad (B26)$$

just by shifting the integration variable for the first term. So, we may add an arbitrary constant to $I_l(k)$ in Eq. (B25), and we choose the constant $-\xi/4\pi$. This will prevent IR divergences in what follows. We are now free to expand $1/(\widetilde{k+p})^2$ to second order in p. After averaging over directions for p, we find

$$\frac{1}{(\widetilde{k+p})^2} - \frac{1}{\widetilde{k}^2} \to p^2\left[\frac{\frac{1}{3}\sum_i\left(\frac{8\sin k_i - \sin 2k_i}{3}\right)^2}{(\widetilde{k}^2)^3}\right.$$

$$\left. - \frac{\frac{1}{3}\sum_i\left(\frac{4\cos k_i - \cos 2k_i}{3}\right)}{(\widetilde{k}^2)^2}\right] \equiv p^2\mathcal{M}(k). \qquad (B27)$$

The equivalent expression in the continuum case is $p^2/3k^4$. Rearranging the terms a little, we can write

$$\frac{C_2}{16\pi^2} = \frac{-1}{24}\int_{k,\mathbb{R}^3-\mathrm{BZ}} \frac{1}{k^5} + \int_{k,\mathrm{BZ}} \frac{1}{8k}\left(\mathcal{M}(k) - \frac{1}{3k^4}\right)$$

$$+ \int_{k,\mathrm{BZ}} \mathcal{M}(k)\left[I_{\mathrm{L}}(k) - \frac{1}{8k} - \frac{\xi}{4\pi}\right]. \qquad (B28)$$

We have seen the first integral. The second gives $(0.031\,075\,769\,5)/16\pi^2$ and the last gives $(0.014\,201\,6)/16\pi^2$; so $C_2 = 0.033\,441\,6$.

Next, we must compute the $O(p^0)$ part of the setting-sun diagram. The continuum diagram is IR and UV logarithmically divergent, while the lattice diagram is only IR logarithmically divergent. It is convenient to IR regulate both by introducing a mass on one line. In this case, the continuum integral may be performed in $\overline{\mathrm{MS}}$, leaving a lattice integral minus an analytically determined counterterm [24,25]. Choosing to separate the renormalization dependence along with the same finite constant as in the previous literature [24,25], the constant C_3 is given by

$$\frac{C_3}{(4\pi)^2} = \lim_{m\to 0}\left\{\int_{k,\text{BZ}}\frac{1}{\widetilde{k}^2+m^2}I_\text{L}(k)-\frac{1}{16\pi^2}\left[\frac{1}{2}+\ln\frac{6}{m}\right]\right\}.$$

(B29)

The problem with this expression is the logarithm. To remove it, we add and subtract $I_\text{C}(k)=1/8k$ to $I_\text{L}(k)$. The integral

$$\int_{k,\text{BZ}}\frac{1}{\widetilde{k}^2+m^2}\left[I_\text{L}(k)-\frac{1}{8k}\right]$$

(B30)

is IR convergent, and the $m\to 0$ limit may be taken immediately. It evaluates to $-(0.068\,584\,32)/16\pi^2$, unless we use the unimproved lattice Laplacian, in which case it is $(0.609\,533\,43)/16\pi^2$. We rearrange the remaining terms to be

$$\int_{k,\text{BZ}}\left(\frac{1}{\widetilde{k}^2+m^2}-\frac{1}{k^2+m^2}\right)\frac{1}{8k}+\int_{k,\text{BZ}}\frac{1}{8k(k^2+m^2)}$$

$$-\frac{1}{16\pi^2}\left[\frac{1}{2}+\ln\frac{6}{m}\right].$$

(B31)

Again, for the first integral the $m\to 0$ limit may be taken immediately, and the numerical value is $(0.161\,799\,607)/16\pi^2$, or $(0.433\,641\,120\,15)/16\pi^2$ if we use the unimproved Laplacian. For the last integral, we cut the integration region into the ball of radius π and the region within the Brillouin zone but outside the ball:

$$\int_{k,\text{BZ}}\frac{1}{8k(k^2+m^2)}=\frac{1}{2\pi^2}\int_0^\pi\frac{k^2dk}{8k(k^2+m^2)}$$

$$+\int_{k,\text{BZ}}\frac{1}{8k(k^2+m^2)}\Theta(|k|-\pi).$$

(B32)

The first integral is easy and gives $\ln(\pi/m)/16\pi^2$ plus terms power suppressed in m. When added to $(-1/16\pi^2)[\ln(6/m)+1/2]$, this cancels the $\ln(m)$, leaving $(1/16\pi^2)[\ln(\pi/6)-1/2]$. The final integral has had the small k part of the integration range removed, so the $m\to 0$ limit is trivial. It may then be reduced to

$$\frac{1}{16\pi^2}\int\frac{d\Omega}{4\pi}\ln\frac{R(\text{cube})}{R(\text{ball})}$$

$$=\frac{1}{16\pi^2}\frac{12}{\pi}\int_0^{\pi/4}d\phi\int_0^{\arctan(\sec\phi)}\sin(\theta)d\theta\ln[\sec(\theta)],$$

(B33)

which numerically equals $(0.192\,335\,131\,95)/16\pi^2$. Note that at no point have we had to deal numerically with an integral that is logarithmically divergent in m, or that still contains m at all.
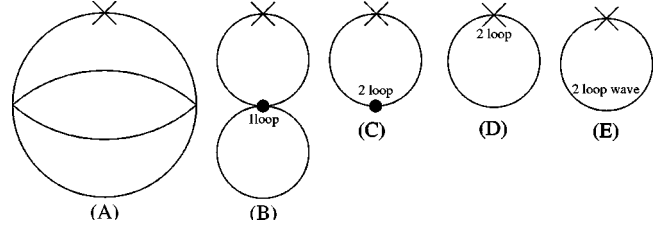

FIG. 19. Three-loop vacuum diagrams needed for $\delta\phi^2$ at three loops. There are seven additional diagrams either involving one loop mass counterterms or tadpoles, which cancel among themselves.

Combining terms gives $C_3=-0.861\,479\,16$, unless we use the unimproved lattice Laplacian, in which case it is $C_{3,\text{U}}=0.088\,480\,10$.

4. Three-loop result for $\delta\phi^2$

In principle, one could extend all the renormalization counterterms we have considered to three-loop order. However, for many of them, this requires including mixing of different dimensions of operator insertions and including counterterms for radiatively induced high-dimension operators in the Lagrangian. However, the three-loop contribution to the additive counterterm $\delta\phi^2$ is an exception: it gives the $O(a)$ corrections to $\Delta\langle\phi^2\rangle_\text{c}$, and we have already seen that we can ignore higher-dimensional operators at this order. The calculation of $\delta\phi^2$ is the least complicated of the three-loop calculations we might envision, and does not require the result of any other three-loop calculations or any of the counterterms that would be needed in a complete three-loop matching. The relevant diagrams are given in Fig. 19. We find

$$\delta\phi_{3l}^2-\delta\phi_{2l}^2=\left[\left(\frac{N+2}{6}\right)^2\xi^2\Sigma+\frac{(N+2)}{18}[C_4-3\Sigma C_1-\Sigma C_2\right.$$

$$\left.+\xi\log(a\bar\mu)]\right]\frac{Nu^2}{(4\pi)^3}-\frac{\xi}{4\pi}Nr.$$

(B34)

Here, the constant C_4 arises from the basketball diagram of Fig. 19, together with part of the mass-squared counterterm diagram. The explicit renormalization scale dependence in Eq. (B34) cancels the implicit dependence of $r=r(\bar\mu)$ in the last term.

Our definition of C_4 is that $[C_4+\xi\log(a\mu)]/(4\pi)^3$ equals the lattice value of the basketball diagram, (A) in Fig. 19, minus diagram (C) taking only the setting-sun part of the two-loop mass counterterm. Explicitly,

$$\frac{C_4+\xi\log(a\mu)}{(4\pi)^3}=\int_{k,\text{BZ}}\frac{1}{(\widetilde{k}^2)^2}\left(\int_{p,\text{BZ}}\frac{1}{p^2}[I_\text{L}(p+k)-I_\text{L}(p)]\right.$$

$$+\int_{p,\mathbb{R}^3}\frac{1}{p^2}I_\text{C}(p)\bigg)$$

$$-\int_{k,\mathbb{R}^3}\frac{1}{k^4}\int_{p,\mathbb{R}^3}\frac{1}{p^2}I_\text{C}(p+k).$$

(B35)

Here, $I_L(p+k)$ and $I_C(p+k)$ arise from the basketball diagram, while $I_L(p)$ and $I_C(p)$ are from the setting-sun piece of the counterterm. Every term here is implicitly IR regulated by a common infinitesimal mass on every propagator, but the way we will perform the integrations means that we will never need this regulation explicitly. Also, continuum integrals are implicitly renormalized in $\overline{\text{MS}}$, which will be relevant.

It is convenient to add and subtract the appropriate factor to put the $I_C(p+k)$ factor inside the BZ k integral. We add and subtract

$$\left[\int_{k,\text{BZ}}\frac{1}{(\widetilde{k}^2)^2}-\int_{k,\mathbb{R}^3}\frac{1}{k^4}\right]\int_{p,\mathbb{R}^3}\frac{1}{p^2}I_C(p+k). \quad \text{(B36)}$$

The p integral may be evaluated in $\overline{\text{MS}}$ (note that we do not need its value in the deep IR where the implicit mass regularization becomes important), and gives

$$\int_{p,\mathbb{R}^3}\frac{1}{p^2}I_C(p+k)=\frac{1.5-\log(k/\mu)}{16\pi^2}. \quad \text{(B37)}$$

The constant terms may be pulled out of the k integrations; the remaining k integral is Eq. (B6) and gives $\xi/4\pi$. The constant parts therefore yield $[1.5+\log(a\mu)]\xi/(64\pi^3)$. The $\ln k$ leads to the integral

$$\frac{1}{16\pi^2}\left(\int_{k,\text{BZ}}\frac{-\ln(ak)}{(\widetilde{k}^2)^2}-\int_{k,\mathbb{R}^3}\frac{-\ln(ak)}{k^4}\right)=\frac{0.308\,37}{64\pi^3} \quad \text{(B38)}$$

for the improved Laplacian. Equation (B35), after subtracting Eq. (B36), becomes

$$\int_{k,\text{BZ}}\frac{1}{(\widetilde{k}^2)^2}\left(\int_{p,\text{BZ}}\frac{1}{\widetilde{p}^2}[I_L(p+k)-I_L(p)]\right.$$
$$\left.-\int_{p,\mathbb{R}^3}\frac{1}{p^2}[I_C(p+k)-I_C(p)]\right). \quad \text{(B39)}$$

It is convenient to split off the part of the continuum p integration that lies outside the Brillouin zone as a separate integration, which does not suffer from divergences,

$$\frac{1}{8}\int_{k,\text{BZ}}\frac{1}{(\widetilde{k}^2)^2}\int_{p,\mathbb{R}^3-\text{BZ}}\left(\frac{1}{p^3}-\frac{1}{p^2|p+k|}\right)=\frac{0.000\,317\,57}{64\pi^3}. \quad \text{(B40)}$$

This leaves as the final integral we must consider,

$$\int_{k,\text{BZ}}\frac{1}{(\widetilde{k}^2)^2}\int_{p,\text{BZ}}\frac{1}{\widetilde{p}^2}[I_L(p+k)-I_L(p)]$$
$$-\frac{1}{p^2}[I_C(p+k)-I_C(p)]\bigg). \quad \text{(B41)}$$

This integration is finite and over a finite integration region (provided we make a prescription that the argument of the p integral is interpreted as the average over p and $-p$ of the quantity written). The integration is nine dimensional and contains some delicate integrable singularities. We find it convenient to use adaptive Monte Carlo integration rather than quadratures. Monte Carlo integration is somewhat problematical when there are integrable singularities. Rather than finding clever changes of variables to get rid of such singularities, the simplest thing to do is to include a small mass in all the propagators (thus, cutting off all singularities), vary that mass, and then numerically extrapolate the zero mass limit from the results of the Monte Carlo integrations. Our result for the integral (B41) is $(0.0985\pm0.006)/(4\pi)^3$. Combining terms, we then have $C_4=0.2817\,(6)$ for the improved Laplacian.

5. Minimalist expression for $\Delta\langle\phi^2\rangle_c$ through $O(a)$

Some of the development in the preceding sections is unnecessary for the isolated goal of getting an $O(a)$ improvement of $\Delta\langle\phi^2\rangle$. It is possible to combine the previous results in the more compact form

$$\Delta\langle\phi^2\rangle_{\text{cont}}=\frac{Z_r}{Z_\phi}\Delta\langle\Phi^2\rangle_{\text{lat}}+\frac{N\xi}{4\pi}ar_1-\frac{N(N+2)}{18}\frac{\mathcal{C}}{(4\pi)^3}au_0^2$$
$$+O(u^3), \quad \text{(B42a)}$$

$$\mathcal{C}\equiv C_4+\xi\ln6+\xi C_3. \quad \text{(B42b)}$$

Here, Φ is the *bare* lattice field, and u_0 the bare lattice coupling, corresponding to the bare lattice action (2.1);

$$\Delta\langle\Phi^2\rangle_{\text{lat}}=\langle\Phi^2\rangle_{\text{lat}}-\frac{N\Sigma}{4\pi a}; \quad \text{(B42c)}$$

r_1 stands for the tadpole-adjusted mass,

$$r_1\equiv r_0+\frac{(N+2)}{6}u_0\frac{\Sigma}{4\pi a}, \quad \text{(B42d)}$$

which is $O(u^2)$ near the transition; and r_0 is the bare mass used in the bare lattice action (2.1). We have retreated from lattice units and explicitly show all factors of a. Since $\Delta\langle\Phi^2\rangle$ is $O(u)$ near the transition, we only need the one-loop result

$$\frac{Z_r}{Z_\phi}\simeq1+\frac{(N+2)}{6}ua\frac{\xi}{4\pi} \quad \text{(B42e)}$$

for Z_r/Z_ϕ.

To finish the relationship between the measurement of $\Delta\langle\phi^2\rangle/u$ and the bare fields and parameters of the lattice Lagrangian, we only need the one-loop relationship between the continuum and bare lattice couplings

$$u_0\simeq u+\frac{(N+8)}{6}u^2a\frac{\xi}{4\pi}. \quad \text{(B42f)}$$

The form (B42) has the conceptual advantage of not introducing the renormalization scale $\bar{\mu}$, since its introduction is unnecessary if one's only interest is in $\Delta\langle\phi^2\rangle_c$ and not the value of r_c. Equation (B42) also makes clear that nothing depends on C_1 and C_2 at this order, so that one does not really need those integrals. And it makes clearer that there is no $O(a^0)$ correction to $\Delta\langle\phi^2\rangle$, which is obscured by Eqs. (2.15) and (2.16). That is,

$$\Delta\langle\phi^2\rangle_{\text{cont}}=\Delta\langle\Phi^2\rangle_{\text{lat}}+O(au^2), \qquad (\text{B43})$$

as in Eq. (2.11).

However, this is not how we have implemented our calculation of $\Delta\langle\phi^2\rangle_c$ when quoting numbers from simulations. What we have done is described in the text and the earlier parts of this appendix and, though equivalent through $O(a)$, will give slightly different numerical values because of differences in higher orders in a.

APPENDIX C: LOGARITHMS IN LARGE-VOLUME SCALING FOR $\alpha=0$

In this section, we review standard renormalization-group arguments about the free energy and verify that a $t^2\ln L$ term appears in the free energy when $\alpha=0$. If one increases renormalization scale by a "blocking" factor of b, the free-energy density of the blocked system is related to the free energy of the original system by a transformation law of the form

$$\mathcal{F}(\{K\})=\mathcal{G}(\{K\})+b^{-d}\mathcal{F}(\{K'\}), \qquad (\text{C1})$$

where $\mathcal{F}$ is the free energy per block, $\{K\}$ represents the couplings of the theory, and $\mathcal{G}$ is an analytic function (depending on b) that represents the contributions to the free energy from the degrees of freedom that have been blocked.[8] Iterating n times, this becomes

$$\mathcal{F}(\{K\})=\sum_{j=0}^{n-1}b^{-jd}\mathcal{G}(\{K^{(j)}\})+b^{-nd}\mathcal{F}(\{K^{(n)}\}), \quad (\text{C2})$$

where $\{K^{(j)}\}$ is the jth iterate of $\{K\}$. If we start with a block size of a and iterate all the way out to size L, we have $n=\log_b(L/a)$.

For t very small but nonzero, the description of the system will first flow towards the critical point, as one blocks to larger and larger distances. But it will then eventually flow away from the fixed point, closely following one of the two unique "outflow" trajectories from the fixed point (one for $t>0$ and one for $t<0$), corresponding to all irrelevant couplings being set to zero. The inhomogeneous part $\mathcal{G}$ of the transformation law (C2) will generate singular behavior as $t\rightarrow 0$, which may then be written as

---

[8]Our presentation follows, for example, chapter 3 of Ref. [26], which is one of many nice introductions to the renormalization group. Our $\mathcal{F}$ and $\mathcal{G}$ are that reference's f and g. We use $\mathcal{F}$ to avoid confusion with f in the text, which was the free energy per physical volume rather than per block.

$$\mathcal{F}(t)\sim\sum_{j=0}^{\log_b(L/a)}b^{-jd}\mathcal{G}(b^{jy_t}t), \qquad (\text{C3})$$

where $b^{jy_t}t$ parametrizes flow along the outflow trajectory. For the infrared behavior at large L and small t, we can replace the sum by an integration. Changing integration variable to $s\equiv b^{jy_t}t$,

$$\mathcal{F}(t)\sim\frac{t^{d/y_t}}{y_t\ln b}\int_t^{t(L/a)^{y_t}}s^{\alpha-3}\mathcal{G}(s)ds, \qquad (\text{C4})$$

where $\alpha=2-d/y_t$. For $\alpha=0$, this is

$$\mathcal{F}(t)\sim\frac{2t^2}{d\ln b}\int_t^{t(L/a)^{d/2}}s^{-3}\mathcal{G}(s)ds. \qquad (\text{C5})$$

To help tame the singularity as $s\rightarrow 0$, integrate by parts two times. This leaves an integral proportional to

$$t^2\int_t^{t(L/a)^{d/2}}s^{-1}\mathcal{G}''(s)ds, \qquad (\text{C6})$$

plus terms that fit the too-naive scaling form (4.12). The remaining integral may be rewritten as

$$\mathcal{G}''(0)t^2\ln(L^{-d/2})+t^2\int_t^{t(L/a)^{d/2}}s^{-1}[\mathcal{G}''(s)-\mathcal{G}''(0)]ds.$$
$$(\text{C7})$$

The second term has the desired analyticity properties of the too-naive scaling form (4.12), and the first term is the logarithm of Privman and Rudnick appearing in Eq. (4.14).

APPENDIX D: OUR OWN ANALYSIS OF C_c

1. Numerical simulation

In this appendix, we discuss our own attempt to determine C_c, to make a crude check of the value we take from Ref. [13]. The scaling of the intersection values $C_\times(L_1,L_2)$ of cumulant curves $C(r)$ is

$$C_\times(L_1,L_2)-C_c\sim\frac{L_1^{y_t}L_2^{-\omega}-L_2^{y_t}L_1^{-\omega}}{L_1^{y_t}-L_2^{y_t}}=\frac{b^{-\omega}-b^{y_t}}{1-b^{y_t}}L_1^{-\omega}$$
$$(\text{D1})$$

for $L_1,L_2\rightarrow\infty$. This is a simple consequence of Binder's analysis [9], but, for the sake of completeness, we briefly outline the argument in Appendix D 2.

We would like to choose L as large as possible, in order to make the scaling law (D1) as accurate as possible, so that we may use it to extrapolate a good value of C_c. Our ultimate interest in this paper is to study continuum O(2) theory, which requires $ua\ll 1$ and for which the scaling limit is $L/a\gg 1/ua$. But $L/a\gg 1/ua$ implies that small ua simulations are an inefficient choice for getting as far as possible into the scaling limit. Because C_c is universal, we may extract it from large ua simulations rather than small ua simulations. [In fact, we could use any model in the same univer-
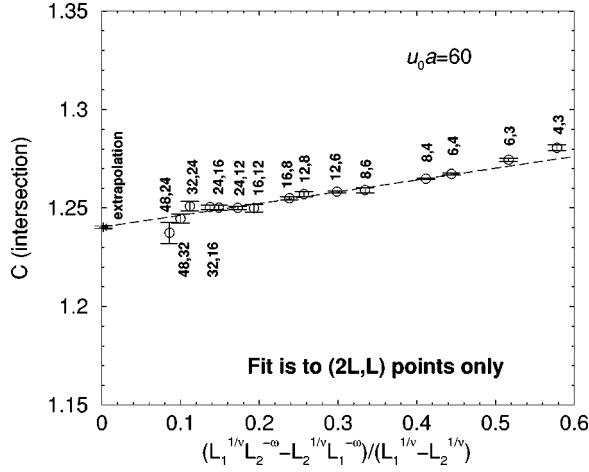
FIG. 20. The values $C_\times(L_1,L_2)$ corresponding to the intersection points of pairs of the curves $C(r)$ for different lattice sizes. The horizontal axis has been chosen so that this relationship should be linear as $L_1,L_2 \to \infty$ (which corresponds to approaching zero on the horizontal axis). Each point is labeled by L_1/a and L_2/a. The linear fit shown is only to that subset of points with $L_1 = 2L_2$.

sality class.] Our simulation code is optimized to perform best if ua is not extremely large, and so we have chosen to extract C_c from data taken with $u_0a = 60$. Because $u_0a = 60$ is not a small value of ua, the $O(a)$ improvements to the action are pointless; unlike other simulations reported in this paper, we quote quantities in terms of the bare lattice parameters.

A variety of intersection values $C_\times(L_1,L_2)$ of $C(r)$ curves are plotted in Fig. 20 against $(L_1^{y_t}L_2^{-\omega} - L_2^{y_t}L_1^{-\omega})/(L_1^{y_t} - L_2^{y_t})$ which, by Eq. (D1), should lead to a linear relationship at large L_1, L_2. The errors on points sharing an L value are correlated, and we compute and use the full correlation matrix for making fits. For the sake of simplicity, however, we have only fit the subset of data with $L_1 = 2L_2$, with results for C_c and the associated confidence levels given in Table II. If we naively include smaller and smaller L until the confidence level of the fit becomes poor, we would fit all the way down to $L = 4$ and obtain

$$C_c = 1.2402(7) \tag{D2}$$

TABLE II. Results of linear fits to the subset of the data of Fig. 20 with $L_1 = 2L_2$, and the corresponding confidence levels ("NA" means not applicable). The first row corresponds to a fit to two points, the second to three points, etc.

Fit	C_c	C.L.
$L_2/a \geqslant 16$	1.229(9)	NA
$L_2/a \geqslant 12$	1.243(4)	6%
$L_2/a \geqslant 8$	1.2404(22)	13%
$L_2/a \geqslant 6$	1.2410(15)	25%
$L_2/a \geqslant 4$	1.2402(7)	35%
$L_2/a \geqslant 3$	1.2394(7)	1%

as our final result. We are suspicious that this result may have a "tail wagging the dog" systematic error. Our small L data has smaller statistical error than our large L data and may be over weighted in the fit to what is supposed to be large L asymptotic behavior. (In particular, in an earlier analysis where we had even poorer statistics on the large L data, we found a result that disagreed even more drastically from the result of Ref. [13].)

2. Large-volume scaling of cumulant intersections

Let us quickly reproduce Binder's result (3.5) for the scaling of $r_\times(L_1,L_2) - r_c$. For large L, we will focus on the scaling piece of the cumulant that, in the notation of Sec. IV A, is

$$C(t,\{u_j\},L^{-1}) \sim C_{\text{sing}}(b^{y_t}t,\{u_jb^{y_j}\},b/L). \tag{D3}$$

Choosing $b = L$,

$$C \simeq C_{\text{sing}}(L^{y_t}t,\{u_jL^{y_j}\},1), \tag{D4}$$

where C_{sing} is a universal scaling function. Now, treat $L^{y_t}t$ and $u_jL^{y_j}$ as small and Taylor expand, keeping track of only the most important irrelevant operator u_j,

$$C \simeq C_{\text{sing}}(0,0,1) + AL^{y_t}t + BL^{-\omega}. \tag{D5}$$

Note that A and $C_{\text{sing}}(0,0,1)$ are universal, but B is not, because it depends on the value of u_j. Now look for the intersection for two different system sizes:

$$C_{\text{sing}}(0,0,1) + AL_1^{y_t}t + BL_1^{-\omega} = C_{\text{sing}}(0,0,1) + AL_2^{y_t}t + BL_2^{-\omega}, \tag{D6}$$

which has solution

$$t \simeq \frac{B(L_1^{-\omega} - L_2^{-\omega})}{A(L_2^{y_t} - L_1^{y_t})} \tag{D7}$$

up to corrections suppressed by additional powers of $1/L$. This is just the scaling (3.5) quoted for $r_\times - r_c$. (And one sees *a posteriori* that it was justified to treat $L^{y_t}t$ as small in the $L \to \infty$ limit.) All that is necessary to derive the scaling (D1) of $C_\times$ is to plug Eq. (D7) back into Eq. (D6) and rename $C_{\text{sing}}(0,0,1)$ as C_c.

In the main text, our procedure for defining the nominal transition in finite volume, for our small ua simulations, is to find the point where $C = C_c$. From Eq. (D6), one may verify that this prescription gives

$$t \simeq \frac{B}{A}L^{-y_t - \omega} \sim L^{-y_t - \omega}, \tag{D8}$$

as asserted in the main text.

APPENDIX E: SMALL Lu EXPANSION OF $\Delta\langle\phi^2\rangle_c$

In this appendix, we compute the expected result for $\Delta\langle\phi^2\rangle_c$ for small volumes in the continuum limit, where we

define the nominal critical temperature in such volumes using Binder cumulants, as explained in Sec. III. We have repeatedly described "short-distance" physics (distance small compared to $1/u$) as perturbative, and so for small volumes ($L \ll 1/u$), one might first try simple perturbation theory to compute $\Delta \langle \phi^2 \rangle$. The leading-order diagram contributing to $\Delta \langle \phi^2 \rangle$ is shown in Fig. 16(d) and corresponds to

$$\langle \phi^2 \rangle \simeq \frac{N}{L^3} \sum_{\mathbf{p}} \frac{1}{p^2 + r}, \qquad (E1)$$

where for the sake of generality we have considered an O(N) model, and the actual case of interest is $N = 2$. The sum is over the discrete momenta $\mathbf{p} = 2\pi \mathbf{n}/L$ associated with the $L \times L \times L$ periodic volume. There is a problem with Eq. (E1), however. Consider the mean-field theory approximation $r_c = 0$ to the critical value of r. The sum then has an infrared divergent term associated with $\mathbf{p} = \mathbf{0}$. The problem is that it is more accurately large-momentum physics that is perturbative, rather than small-distance physics. So, even when $L \rightarrow 0$, the physics associated with the $\mathbf{p} = \mathbf{0}$ modes is nonperturbative. Since this is only one mode, we simply analyze it separately, and then treat all the $\mathbf{p} \neq \mathbf{0}$ modes perturbatively.

1. The case $r = 0$: Leading order

To illustrate the calculation, let us first compute $\Delta \langle \phi^2 \rangle$ if $r = 0$. We'll later come back to consider the actual r that is chosen by the criteria of our simulations that the cumulant $C = C_c$. Consider the approximation S_0 to the action where we ignore everything but the $\mathbf{p} = \mathbf{0}$ modes ϕ_0

$$S_0 = \int d^3 x \left[|\nabla \phi_0|^2 + \frac{u}{4!} |\phi_0|^4 \right] = \frac{L^3 u}{4!} |\phi_0|^4. \quad (E2)$$

Note that this result holds on the lattice as well as in the continuum. The $\mathbf{p} = \mathbf{0}$ contribution to $\Delta \langle \phi^2 \rangle$ is then

$$\langle \phi_0^2 \rangle \simeq \frac{\int d^N \phi_0 e^{-S_0} |\phi_0|^2}{\int d^N \phi_0 e^{-S_0}} = \left(\frac{4!}{L^3 u} \right)^{1/2} \frac{\int d^N x e^{-x^4} x^2}{\int d^N x e^{-x^4}}$$

$$= \left(\frac{4!}{L^3 u} \right)^{1/2} \frac{\Gamma\left(\dfrac{N+2}{4}\right)}{\Gamma\left(\dfrac{N}{2}\right)}. \qquad (E3)$$

By dimensional analysis, the leading perturbative contribution of the $\mathbf{p} \neq \mathbf{0}$ modes to $\langle \phi^2 \rangle$ should be order L^{-1} and so is dominated by the zero-mode contribution (E3). Specializing to $N = 2$, we then have

$$\frac{\langle \phi^2 \rangle_{r=0}}{u} = \sqrt{\frac{4!}{(Lu)^{3/2}}} + O((Lu)^{-1})$$

$$\simeq \frac{2.763\,95}{(Lu)^{3/2}} + O((Lu)^{-1}). \qquad (E4)$$

As we will see explicitly below, the UV subtraction that converts $\langle \phi^2 \rangle$ to $\Delta \langle \phi^2 \rangle$ in the continuum limit is not relevant until next order in $(Lu)^{-1}$, and so $\Delta \langle \phi^2 \rangle / u$ also has the expansion (E4).

2. The case $r = 0$: Next-to-leading order

Now, consider the leading-order perturbative contribution $\delta \langle \phi^2 \rangle$ of the nonzero modes to $\langle \phi^2 \rangle$ from Eq. (E1),

$$\delta \langle \phi^2 \rangle \simeq \frac{N}{L^3} \sum_{\mathbf{p} \neq 0} \frac{1}{p^2}. \qquad (E5)$$

This sum is UV divergent, and the UV divergence is simply the free-field divergence discussed in Sec. (II A). It is subtracted when we compute $\Delta \langle \phi^2 \rangle$ as opposed to $\langle \phi^2 \rangle$. Note that our prescriptions (2.11) or (2.15) for computing $\Delta \langle \phi^2 \rangle$ in our simulations involve subtracting the *infinite volume* free-field result for $\langle \phi^2 \rangle$. In the continuum limit, this subtraction turns the perturbation (E5) into

$$\delta \Delta \langle \phi^2 \rangle = \frac{N}{L^3} \sum_{\mathbf{p} \neq 0} \frac{1}{p^2} - N \int_{\mathbf{p}} \frac{1}{p^2}$$

$$= \frac{N}{(2\pi)^2 L} \left[\sum_{\mathbf{n} \neq 0} \frac{1}{n^2} - \int \frac{d^3 n}{n^2} \right]. \qquad (E6)$$

Individually, the sums and integrals above must be consistently regulated, for example, by dimensional regularization or by keeping the system on a lattice with arbitrarily small lattice spacing.

There are a number of ways to evaluate the result numerically. One is to start by regulating with dimensional regularization, working in d spatial dimensions. Then

$$\delta \Delta \langle \phi^2 \rangle = \frac{N}{L^d} \sum_{\mathbf{p} \neq 0} \frac{1}{p^2} - N \int_{\mathbf{p}} \frac{1}{p^2} \qquad (E7)$$

$$= \frac{N}{(2\pi)^2 L^{d-2}} \left[\sum_{\mathbf{n} \neq 0} \frac{1}{n^2} - \int \frac{d^d n}{n^2} \right].$$

Now rewrite

$$\frac{1}{n^2} = \int_0^\infty ds\, e^{-sn^2}. \qquad (E8)$$

The n_1, n_2, ..., sums and integrals then factor, giving

$$\sum_{\mathbf{n} \neq 0} \frac{1}{n^2} - \int \frac{d^d n}{n^2} = \int_0^\infty ds \left\{ [\theta_3(e^{-s})]^d - 1 - \left(\frac{\pi}{s}\right)^{d/2} \right\}, \qquad (E9)$$

where

$$\theta_3(q) \equiv \sum_{k=-\infty}^{\infty} q^{-(k^2)} \qquad (E10)$$

is a special case of an elliptic theta function. The integral on the right-hand side of Eq. (E9) is absolutely convergent in

$d=3$, so we may now dispense with dimensional regularization and set d to three. The integral is then easily done numerically, giving

$$\sum_{\mathbf{n}\neq 0}\frac{1}{n^2}-\int\frac{d^d n}{n^2}\simeq -8.913\,63. \qquad (E11)$$

For $N=2$, one then has

$$\frac{\delta\Delta\langle\phi^2\rangle_{r=0}}{u}\simeq -\frac{0.451\,570}{Lu}. \qquad (E12)$$

The effect of interactions in the nonzero mode sector will be perturbative for small Lu and will give higher-order contributions to $\Delta\langle\phi^2\rangle$. However, we must also consider interactions of the zero mode ϕ_0 with the nonzero modes, which will give corrections to the action S_0 used in our earlier analysis of ϕ_0. For instance, the coupling u in S_0 will pick up corrections of order Lu^2. This will generate an $O(Lu)$ relative correction to the zero-mode contribution (E4), and so that correction will be higher order than the contribution (E12) computed above. A similar story will hold for corrections to r (and for the effects of higher-dimensional interactions) with the complication that r will receive some infinite contributions in the continuum limit, corresponding to the usual mass renormalization. The latter is absorbed by the usual renormalization of r, and so one has

$$\frac{\delta\langle\phi^2\rangle_{r=0}}{u}\simeq \frac{2.763\,95}{(Lu)^{3/2}}-\frac{0.451\,570}{Lu}+O((Lu)^{-1/2}) \qquad (E13)$$

if one interprets the r in the condition $r=0$ as being renormalized r. (The details of the renormalization scheme will not matter at the order shown.)

3. The case $C=C_c$

Now, instead of setting $r=0$, we will choose r so that the cumulant C is equal to its critical value. Let us begin with a leading-order analysis and so focus on just the $\mathbf{p}=\mathbf{0}$ sector. For general r, we then have

$$S_0=\frac{L^3 r}{2}|\phi_0|^2+\frac{L^3 u}{4!}|\phi_0|^4 \qquad (E14)$$

and

$$\langle\phi_0^{2k}\rangle=\frac{\int d^N\phi_0 e^{-S_0}|\phi_0|^{2k}}{\int d^N\phi_0 e^{-S_0}}. \qquad (E15)$$

By a change of variables, this may be rewritten as

$$\langle\phi_0^{2k}\rangle=\left(\frac{4!}{L^3 u}\right)^{k/2}\frac{I_k(R)}{I_0(R)} \qquad (E16)$$

where

$$I_k(R)\equiv\int_0^{\infty}dy\,e^{-y^2-Ry}y^{k+(N-2)/2}, \qquad (E17)$$

and

$$R\equiv\frac{r}{2}\left(\frac{4!L^3}{u}\right)^{1/2}. \qquad (E18)$$

Now note that the volume average $\bar{\phi}$ of the field, used in the definition of the cumulant, is simply ϕ_0. Specializing now to $N=2$ and doing the I_k integrals, one obtains

$$I_0(R)=\frac{\sqrt{\pi}}{2}e^{R^2/4}\mathrm{erfc}\left(\frac{R}{2}\right), \qquad (E19)$$

$$I_1(R)=\frac{1}{2}[1-RI_0(R)], \qquad (E20)$$

$$I_2(R)=\frac{1}{4}[-R+(R^2+2)I_0(R)]. \qquad (E21)$$

The cumulant may be written

$$C\equiv\frac{\langle\phi_0^4\rangle}{\langle\phi_0^2\rangle^2}\simeq\frac{I_2(R)I_0(R)}{[I_1(R)]^2}. \qquad (E22)$$

A numerical search for the point where $C=C_c\simeq 1.243$ gives

$$R\simeq -2.5073. \qquad (E23)$$

At this R, the zero-mode contribution to $\langle\phi^2\rangle$ is then

$$\langle\phi^2\rangle_c=\left(\frac{4!}{L^3 u}\right)^{1/2}\frac{I_1(R)}{I_0(R)}+O((Lu)^{-1})$$

$$=\frac{6.440\,03}{(L^3 u)^{1/2}}+O((Lu)^{-1}). \qquad (E24)$$

Since the result for R is a pure number, the definition (E18) of R shows that r is of order $\sqrt{u/L^3}$, which is smaller by a power of $\sqrt{Lu}$ than any nonzero momentum squared, which are order L^{-2}. So r may be ignored in finding the leading contribution of the nonzero modes, with the effect that $\delta\Delta\langle\phi^2\rangle$ is the same as in the earlier $r=0$ analysis. Adding Eqs. (E24) and (E12) then produces the result (4.15) quoted in the main text.

APPENDIX F: SYSTEM SIZE AND THE SIMULATIONS OF GRÜTER *et al.*

One of the applications of O(2) field theory is to studying the corrections to the critical temperature, due to interactions, for Bose-Einstein condensation of a nearly ideal nonrelativistic Bose gas. This application has been previously studied using numerical techniques. Our discussion of system size in Sec. IV C has implications for an early study by Grüter *et al.* [22], which is that much of the data collected was perhaps in insufficiently large volume. These simulations did not make use of O(2) field theory: They worked in

the canonical ensemble and studied the path integral for a fixed number N_p of particles in a finite volume V. If no attempt were made to fit for large-volume corrections, then Fig. 2 makes it clear that one should take roughly $Lu \gtrsim 400$ to keep those corrections moderately small. It is illuminating to also consider the less restrictive condition of roughly $Lu \gtrsim 200$. We may translate these conditions on system size to the context of Bose-Einstein condensation by translating the parameter u of the O(2) field theory. For this application, the relation is [2] $u = 96\pi^2 a/\lambda^2$, where a is the scattering length of the atoms, $\lambda = \hbar\sqrt{2\pi/mk_B T}$ is the thermal wavelength, and m is the mass of the atoms. Using the ideal gas approximation $T_c \simeq T_0 = (2\pi\hbar^2/k_B m)[n/\zeta(3/2)]^{2/3}$ for the critical temperature, one may write

$$na^3 \simeq \left(\frac{Lu}{96\pi^2}\right)^3 \frac{\zeta\left(\frac{3}{2}\right)^2}{N_p} \qquad (\text{F1})$$

at the transition. The conditions $Lu \gtrsim 400$ or 200 may then be translated into the conditions

$$na^3 \gtrsim \frac{0.51}{N_p} \quad \text{or} \quad \frac{0.064}{N_p}. \qquad (\text{F2})$$

The largest N_p used in the simulations of Grüter *et al.* was $N_p = 216$, and their extraction of the critical temperature depended on results with $N_p = 125$ as well. For the latter, our rough conditions for being in large enough volume then requires $na^3 \gtrsim 0.004$ or 0.0005, depending on whether one takes the more or less restrictive condition $Lu \gtrsim 400$ or $Lu \gtrsim 200$. Grüter *et al.* quote results for na^3 all the way down to 10^{-5}, and the majority of points in their small na^3 tail have $na^3 \lesssim 10^{-4}$. (See Fig. 3 of Ref. [22].) It therefore seems at least possible that they may have had inadequate system sizes for their extrapolation of the $ua \to 0$ behavior.

[1] P. Arnold and G. Moore, Phys. Rev. Lett. **87**, 120401 (2001).

[2] G. Baym, J.-P. Blaizot, M. Holzmann, F. Laloë, and D. Vautherin, Phys. Rev. Lett. **83**, 1703 (1999).

[3] D. Bedingham and T. Evans, e-print hep-ph/0011286.

[4] P. Arnold and S. Tkachenko, Phys. Rev. D **64**, 105018 (2001).

[5] P. Arnold and B. Tomášik, Phys. Rev. A **64**, 053609 (2001).

[6] G. Watson, Quarterly J. Math. **10**, 266 (1939).

[7] M. Holzmann, G. Baym, J.-P. Blaizot, and F. Laloë, Phys. Rev. Lett. **87**, 120403 (2001).

[8] J. Goodman and A.D. Sokal, Phys. Rev. Lett. **56**, 1015 (1986); J. Goodman and A.D. Sokal, Phys. Rev. D **40**, 2035 (1989).

[9] K. Binder, Phys. Rev. Lett. **47**, 693 (1981); Z. Phys. B: Condens. Matter **43**, 119 (1981).

[10] J.A. Lipa, D.R. Swanson, J.A. Nissen, T.C.P. Chui, and U.E. Israelsson, Phys. Rev. Lett. **76**, 944 (1996).

[11] J.A. Lipa, D.R. Swanson, J.A. Nissen, Z.K. Geng, P.R. Williamson, D.A. Stricker, T.C.P. Chui, U.E. Israelsson, and M. Larson, Phys. Rev. Lett. **84**, 4894 (2000).

[12] R. Guida and J. Zinn-Justin, J. Phys. A **31**, 8103 (1998).

[13] M. Campostrini, M. Hasenbusch, A. Pelissetto, and P. Rossi, Phys. Rev. B **63**, 214503 (2001).

[14] M. Hasenbusch and T. Török, J. Phys. A **32**, 6361 (1999).

[15] H.W.J. Blöte, E. Luijten, and J.R. Heringa, J. Phys. A **28**, 6289 (1995).

[16] M. Fisher, Phys. Rev. **176**, 257 (1968).

[17] M. N. Barber, in *Phase Transitions and Critical Phenomena*, edited by C. Domb and J. L. Lebowitz (Academic Press, New York, 1983), Vol. 8.

[18] V. Privman and M.E. Fisher, Phys. Rev. B **30**, 322 (1984).

[19] V. Privman and J. Rudnick, J. Phys. A **19**, L1215 (1986).

[20] G. Baym, J.-P. Blaizot, and J. Zinn-Justin, Europhys. Lett. **49**, 150 (2000).

[21] P. Arnold and B. Tomášik, Phys. Rev. A **62**, 063604 (2000).

[22] P. Grüter, D. Ceperley, and F. Laloë, Phys. Rev. Lett. **79**, 3549 (1997).

[23] G.D. Moore, Nucl. Phys. B **493**, 439 (1997); **523**, 569 (1998).

[24] K. Farakos, K. Kajantie, K. Rummukainen, and M. Shaposhnikov, Nucl. Phys. B **442**, 317 (1995).

[25] M. Laine and A. Rajantie, Nucl. Phys. B **513**, 471 (1998).

[26] J. Cardy, *Scaling and Renormalization in Statistical Physics* (Cambridge University Press, Cambridge, 1997).